TURUN YLIOPISTON JULKAISUJA
ANNALES UNIVERSITATIS TURKUENSIS

SARJA - SER. A I OSA - TOM. 464

ASTRONOMICA - CHEMICA - PHYSICA - MATHEMATICA

NON-MARKOVIAN DYNAMICS AND QUANTUM INFORMATION PROBES

by

Pinja Haikka

TURUN YLIOPISTO
UNIVERSITY OF TURKU
Turku 2013

From

Department of Physics
University of Turku
Finland

Supervised by

Sabrina Maniscalco
Docent
Department of Physics
and Astronomy
University of Turku
Finland

Reader
School of Engineering
and Physical Sciences
Heriot-Watt University
Scotland

Reviewed by

Heinz-Peter Breuer
Professor
Physikalisches Institut
Universität Freiburg
Germany

Carlos Pineda
Professor
Instituto de Física,
Universidad Nacional Autónoma de México
Mexico

Opponent

Susana Huelga
Professor
Institute of Theoretical Physics
Ulm University
Germany

ISBN 978-951-29-5447-6
ISBN 978-951-29-5448-3
ISSN 0082-7002
Painosalama Oy - Turku, Finland 2013

Acknowledgments

Without a doubt I am most indebted to my wonderful supervisor Sabrina, whose contagious enthusiasm has been an invaluable source of motivation during my doctoral studies. I could not imagine a better training to become a physicist than the five years I have spent with her, nor a more stimulating environment than our group with its multitude of inspiring activities.

A very big thank you also to all the members, both past and present, of the group for numerous interesting discussions and fun moments throughout the years. It is a luxury to be able to work daily with such a great collection of people.

At the University of Turku, my long time academic home, I wish to thank Kalle-Antti, Jyrki and all the people of our corridor for creating an atmosphere that makes work a pleasure. A special thanks to Elsi, who has been my comrade since the very first year of university and shared with me the ups and downs of this long journey.

I wish to thank all of my collaborators over the years for sharing their knowledge with me and introducing me to new and exciting topics in physics. Thank you to Jim for hosting me in Sydney, to Vlatko for inviting me to spend two months in Singapore and introducing me to John, Kavan and a bunch of other great people, and to Fernando, Marcelo and Luiz for their hospitality in Brazil.

When I started my PhD, I never expected to end up having so many friends all over the world. I have been lucky to meet such a collection of exceptional people and to share so many special moments with them.

Finally, thank you to my friends, family and especially to Janne for supporting me, taking my mind off physics when necessary and for making sure I also have a life in the classical world.

Contents

Abstract

This Thesis discusses the phenomenology of the dynamics of open quantum systems marked by non-Markovian memory effects. Non-Markovian open quantum systems are the focal point of a flurry of recent research aiming to answer, e.g., the following questions: What is the characteristic trait of non-Markovian dynamical processes that discriminates it from forgetful Markovian dynamics? What is the microscopic origin of memory in quantum dynamics, and how can it be controlled? Does the existence of memory effects open new avenues and enable accomplishments that cannot be achieved with Markovian processes? These questions are addressed in the publications forming the core of this Thesis with case studies of both prototypical and more exotic models of open quantum systems.

In the first part of the Thesis several ways of characterizing and quantifying non-Markovian phenomena are introduced. Their differences are then explored using a driven, dissipative qubit model. The second part of the Thesis focuses on the dynamics of a purely dephasing qubit model, which is used to unveil the origin of non-Markovianity for a wide class of dynamical models. The emergence of memory is shown to be strongly intertwined with the structure of the spectral density function, as further demonstrated in a physical realization of the dephasing model using ultracold quantum gases.

Finally, as an application of memory effects, it is shown that non-Markovian dynamical processes facilitate a novel phenomenon of time-invariant discord, where the total quantum correlations of a system are frozen to their initial value. Non-Markovianity can also be exploited in the detection of phase transitions using quantum information probes, as shown using the physically interesting models of the Ising chain in a transverse field and a Coulomb chain undergoing a structural phase transition.

List of articles

This thesis consists of an introductory review and the following nine articles [1–9]:

I P. Haikka,
Non-Markovian master equation for a damped driven two-state system,
Phys. Scr. T140, 014047 (2009).

II P. Haikka and S. Maniscalco,
Non-Markovian dynamics of a damped driven two-state system
Phys. Rev. A 81, 052103 (2010).

III P. Haikka, J. D. Cresser and S. Maniscalco
Comparing different non-Markovianity measures: A case study
Phys. Rev. A 83, 012112 (2011).

IV P. Haikka, S. McEndoo, G. De Chiara, M. Palma and S. Maniscalco
Quantifying, characterizing and controlling information flow in ultracold atomic gases
Phys. Rev. A 84, 031602(R) (2011).

V P. Haikka, J. Goold, S. McEndoo, F. Plastina and S. Maniscalco
Non-Markovianity, Loschmidt echo and criticality: A unified picture
Phys. Rev. A 85, 060101(R) (2012).

VI P. Haikka, S. McEndoo, G. De Chiara, M. Palma and S. Maniscalco
Robust non-Markovianity in ultracold gases
Phys. Scr. T151, 014060 (2012).

VII P. Haikka, T. H. Johnson and S. Maniscalco
Non-Markovianity of local dephasing channels and time invariant discord
Phys. Rev. A 87, 010103(R) (2013).

VIII P. Haikka, S. McEndoo and S. Maniscalco
Non-Markovian probes in ultracold gases
Phys. Rev. A 87, 012127 (2013).

IX M. Borrelli, P. Haikka, G. De Chiara and S. Maniscalco
Non-Markovian qubit dynamics induced by Coulomb crystals
Submitted for publication, arXiv:1302.4260.

Other published material

This is a list of the publications produced which have not been chosen as a part of the doctoral thesis [10, 11].

- S. McEndoo, P. Haikka, G. De Chiara, M. Palma and S. Maniscalco
  Entanglement control via reservoir engineering in ultracold atomic gases
  Europhys. Lett. 101, 60005 (2013).

- C. Addis, P. Haikka, S. McEndoo, C. Macchiavello and S. Maniscalco
  Two-qubit non-Markovianity induced by a common dephasing environment
  Phys. Rev. A 87, 052109 (2013).

Chapter 1

Introduction

The theory of open quantum systems touches all subfields of quantum physics due to the profound fact that no system is ever truly isolated from its surroundings [12–14]. Open systems theory asserts that the standard description of quantum mechanics in terms of pure states and unitary operations is an idealisation, valid at best on the level of an approximation. Besides complicating the mathematical formulation of quantum physics, the effect of environmental noise is to strip a system from its quantumness by destroying quantum superpositions and entanglement, the two main characteristic features of quantum systems not found in the classical world. Indeed, the quantum-to-classical transition is often attributed to decoherence arising from quantum systems evolving under the influence of an environment [15]. This makes the study of open systems very topical: it is important to understand thoroughly how environmental noise affects quantum physics on the level of both foundations and applications.

The effect of the environment on the dynamics of an open system is to replace unitary evolution with non-unitary dynamics. Mathematically this is described by completely positive and trace preserving maps, the most general transformations that can be done to a quantum state. Dynamical maps are conventionally classified into two major categories: those describing Markovian memoryless dynamics and those whose evolution is characterized by memory effects, coined *non-Markovian* maps. The latter ones are marked by revivals of information and/or energy that temporarily combat the detrimental effect of the environment, prolonging the existence of quantum properties. Moreover, Markovian dynamics is often only an approximation of the more realistic and more complicated non-Markovian dynamics, and the simple Markovian description fails if applied to complex system-environment interactions where memory effects become important.

The fundamental importance of non-Markovian open system dynamics is widely acknowledged these days, but in the past the whole concept has lacked a simple, model-independent definition. While Markovianity is well defined for classical stochastic processes, the formal definition does not translate straightforwardly into the language of quantum physics. The line dividing the two classes is still elusive and subject to active ongoing debate. Attempts to generalize the notion of a Markovian process to the quantum domain has lead to a multitude of subtly different definitions for non-Markovianity, but a consensus is still missing: should the characteristic feature of (non-)Markovian dynamics be a mathematical property of the dynamical map, or is it captured by the way a relevant quantity evolves in time?

The state-of-the-art of defining non-Markovian open quantum systems is reviewed in Ch. 2 with a focus on two prevailing non-Markovianity measures. The figure of merit of the first measure, advocated by Rivas, Huelga and Plenio (RHP), is the so-called *divisibility* property of the dynamical map. Divisibility intuitively corresponds to memoryless dynamics and non-Markovianity can be quantified as the degree of deviation from a divisible map [16]. An alternative approach, proposed by Breuer, Laine and Piilo (BLP), is based on information flux [17, 18]. The effect of the environment on the quantum system is to reduce the distinguishability of quantum states in time, associated to a loss of information about the quantum system. Non-Markovianity is identified as a process with bidirectional information flux, revealed as intervals of time when the distinguishability of two quantum states temporarily increases, and quantified as the maximal amount of information that the system can recover during its time-evolution. These two definitions do not agree for all quantum processes, and in Ch. 2 I present a case study of a simple but non-trivial physical model, a driven two-level atom in a dissipative environment, where these differences are explored.

The application of non-Markovianity quantifiers has led to a deeper understanding of dynamics characterized by memory. For example, it is now well established that the form of the equations of motion of a quantum system is not necessarily relevant when assessing non-Markovianity: on one hand, time-local master equations can describe non-Markovian dynamics exactly, and on the other hand, memory kernel master equations may lead to forgetful dynamics [19]. Recently, the possibility of exploiting non-Markovianity has been considered in various scenarios and so far non-Markovianity has been linked, for example, to an increase in the amount of steady-state entanglement [20] and to improvements in quantum metrology

[21]. In the context of quantum information protocols non-Markovianity has been shown to be a resource for quantum key distribution [22] and teleportation [23], and to increase quantum channel capacity [24]. The role of memory effects has also been studied in the context of chaotic dynamics [25, 26] and biological systems [27, 28]. Finally, experiments measuring non-Markovianity in a linear optics set-up have established that non-Markovianity quantifiers are not merely a theoretical tool [29].

Despite the advances already made, many questions still remain unexplored. In this Thesis I focus on two general problems via case studies on specific physical models. The first question is how non-Markovian phenomena emerges. With rigorous definitions of non-Markovianity at hand the origin of non-Markovianity, for certain classes of physical models, can be traced back to specific microscopic features of the model. In Ch. 3 I introduce a condition on the spectral density function of a general dephasing model to induce non-Markovian dynamics. The question is revisited in Ch. 4 in the context of a physically realizable dephasing model where we show how the environment can be suitably tailored to induce non-Markovian dynamics. We also reveal that the connection between the form of the spectral density function and non-Markovianity is more subtle than initially anticipated.

The second core question of the Thesis is how non-Markovianity can be utilized in certain situations. An interesting result in this direction is the existence of *time-invariant discord*, presented in Ch. 3. Quantum discord is a measure for total quantum correlations in a quantum state, exceeding those captured by entanglement [30–32]. We discovered a class of non-Markovian dynamical maps that leave quantum discord invariant in time even though other physical quantities including entanglement decay continuously. This phenomenon is particularly interesting in light of very recent results [33], linking frozen values of quantum and classical correlations to the emergence of pointer states and the quantum-to-classical transition [34]. We further show that the class of dynamical maps facilitating time-invariant discord is exactly those for which the Markovian approximation fails, making it an inherently non-Markovian dynamical feature.

In Ch. 5 I discuss a novel way to exploit non-Markovianity measures by using a qubit to probe a large quantum many-body system, which acts as an environment for the qubit. The way the qubit evolves depends on the properties of the the many-body system; conversely, some of these properties can be inferred from the qubit dynamics. We have shown that a fundamental dynamical quantity describing the sensitivity of a many-body system

to external perturbations, the *Loschmidt echo* [35], is directly linked to the way a probe qubit dephases, and that the degree on non-Markovianity of the probe qubit dynamics can be expressed in terms of the Loschmidt echo only. Decay of the Loschmidt echo is enhanced at criticality, and with the link established between the Loschmidt echo and non-Markovianity of the probe qubit we discovered that a phase transition of the environment can be unambiguously manifested in the qubit dynamics. In Ch. 5 I present schemes for detecting the phase transitions of two physically interesting models, the transverse Ising model and a Coulomb crystal, by observing the non-Markovian dynamics of a probe qubit.

The Thesis is structured as follows. Chapter 2 is an introduction to the topic of defining and quantifying non-Markovian phenomena. After a short summary of the measures proposed recently I specify the discussion to a physical model, the driven qubit, to concretely demonstrate how the two prevailing measures can be computed and how they differ from each other. After formally introducing the concept of non-Markovianity I focus on the two major themes of the Thesis, namely how non-Markovianity emerges and how it can be exploited. Chapter 3 is dedicated to exploring these issues in the context of a general dephasing qubit model. This exactly solvable model is an ideal testbed for addressing the microscopic origin of non-Markovianity in a general setting, and shows an interesting consequence of the failure of the Born-Markov approximation, the phenomenon of time-invariant discord. In Ch. 4 I discuss how the general dephasing model could be realized in a laboratory using ultracold atomic gases. Besides presenting an experimentally realistic scenario where the predictions of Ch. 3 could be tested, a detailed study of slightly different realizations of the dephasing model reveals a surprising connection between the structure of the reservoir and (non-)Markovianity of the qubit. Chapter 5 introduces the concept of a non-Markovian probe qubit, that is, a qubit able to probe some important properties of a many-body system. The properties are reflected in the (non-)Markovianity of the qubit, as demonstrated in a striking way when probing two different critical many-body systems. Finally, Ch. 6 concludes and summarizes the Thesis.

Chapter 2

Non-Markovian processes

Quantum systems are never isolated from their surroundings and the theory of closed quantum systems fails to describe many essential features of quantum dynamics. It is therefore necessary to include the effect of the environment in the dynamical description of the quantum system. The theory of open quantum systems describes how an environment modifies the properties of a quantum system.

Including the environment in the equation of motion introduces a large, typically infinite, number of degrees of freedom, complicating tremendously the description of the system. Furthermore, one is typically not interested in the dynamics of the environment but rather on its effects on the system. For this reason it it useful to reduce the description of the total closed system to the description of the system of interest only. In this framework the system states are generally described as mixed states, while the composite system-environment state is assumed to be pure and evolving unitarily. The dynamics of open systems is constructed as follows:

1. For an initial time t_0 assign an environment state ξ to the system state:
$$\rho(t_0) \equiv \rho_0 \mapsto \rho_0 \otimes \xi.$$

2. Let the composite system evolve unitarily for a period of time t:
$$\rho_0 \otimes \xi \mapsto U_t(\rho_0 \otimes \xi)U_t^\dagger.$$

3. Trace out the environmental degrees of freedom:
$$U_t(\rho_0 \otimes \xi)U_t^\dagger \mapsto \mathrm{Tr}_E\{U_t(\rho_0 \otimes \xi)U_t^\dagger\} \equiv \rho(t).$$

The dynamical map

$$\Phi_{t_0,t}:\ \rho(t_0) \mapsto \rho(t) = \Phi_{t_0,t}\rho(t_0) \tag{2.1}$$

arising from this construction preserves the trace and positivity of the system state. The map is also completely positive (CP) and therefore it describes the most general transformation in the space of physical states. Moreover, Stinespring's dilation theorem states that all trace preserving CP maps can be constructed in this way, i.e., by extending their evolution to unitary dynamics in a larger Hilbert space [36], emphasizing the generality of this construction.

While the construction elaborated above gives, in principle, the dynamical map exactly, the form of the map is often too complicated to handle. In fact, many approaches for resolving the system dynamics give the reduced system dynamics in terms of the *master equation*,

$$\frac{d\rho(t)}{dt} = \mathcal{L}_t\rho(t), \tag{2.2}$$

that is, an equation of motion for the state $\rho(t)$ determined by the time-dependent superoperator $\mathcal{L}_t$. The master equation derivation is formalized by Nakajima-Zwanzig [37] and time-convolutionless [38] projection operator techniques. In practice, the master equation can be obtained by tracing out the environmental degrees of freedom from the von-Neumann equation of the composite system-environment state:

$$\frac{d\rho(t)}{dt} = -i\mathrm{tr}_E\{[H, \rho_{SE}(t)]\}, \tag{2.3}$$

where

$$\rho(t) = \mathrm{tr}_E\{\rho_{SE}(t)\} \tag{2.4}$$

is the state of the system of interest and $\rho_{SE}(t)$ the state of the total system, typically assumed to be initially of the factorized form $\rho_{SE}(t_0) = \rho_S(t_0) \otimes \rho_E(t_0)$, and H is the total Hamiltonian. Master equation (2.3) is exact, but typically too involved to treat sensibly, and therefore a number of approximations has to be implemented to arrive at a master equation that is easier to handle.

The commonly employed Born approximation assumes weak system-environment coupling and amounts to treating the master equation perturbatively, typically up to second order in the system-environment coupling.

Another typical approximation is the Markov approximation, which neglects reservoir memory effects and is valid when the time-scale characterizing the decay of reservoir correlation functions is very short in comparison to all other dynamical time-scales characterizing the system dynamics. Within these two approximations the master equation takes the famous Lindblad form [39, 40]:

$$\frac{d\rho(t)}{dt} = -i[H_S, \rho(t)] + \sum_k \gamma_k \left[A_k \rho(t) A_k^\dagger - \frac{1}{2} \left\{ A_k^\dagger A_k, \rho(t) \right\} \right], \tag{2.5}$$

where $\gamma_k \geq 0$ are the *decay rates* and A_k the corresponding *jump operators*. Loosely speaking this equation describes the statistics of a dynamical process where the unitary dynamics of the system, described by an effective system Hamiltonian H_{eff}, is disrupted by abrupt changes, *quantum jumps*. The jumps are characterized by operators A_k and the decay rate γ_k relates to the probability of the jump occurring during a given time interval [41,42].

The dynamical map corresponding to the Lindblad master equation has two interesting properties: it is time-homogenous,

$$\Phi_{t_0,t} = \Phi_{t-t_0,0} \equiv \Phi_\tau, \tag{2.6}$$

where $\tau = t - t_0$, and it obeys the *semi-group property*,

$$\Phi_{t+s} = \Phi_t \Phi_s. \tag{2.7}$$

The semi-group property means that the map can be divided into infinitely many time-steps, each identical and independent of the past and future steps [43], and therefore the dynamical map has the intuitive interpretation of memoryless dynamics. Memoryless dynamics is strongly intertwined with the Markov approximation and much of the theory of non-Markovian open quantum systems revolves around understanding how relaxing the Markov approximation affects the form of the master equation and the corresponding dynamical map, how this translates to the dynamical properties of the system of interest, and when and why the Markov approximation is no longer valid.

2.1 Defining non-Markovianity

The Lindblad master equation is universally accepted as the prototype of Markovian, memoryless dynamics, prompted by the semi-group property

which implies that future evolution of the state is independent of the past states. Discrepancies arise when addressing the question of what is *not* Markovian and, to date, a plethora of deviating points of view have been advocated. While all Markovian maps resemble one another, each non-Markovian map is non-Markovian in its own way. In this Section I introduce the concept of non-Markovian dynamics more quantitatively and present several prevailing non- Markovianity measures that quantify the degree of non-Markovianity in a quantum process.

In a microscopic derivation of Eq. (2.5) the semi-group property follows from the Markov approximation but it is, in fact, a characteristic of *all* dynamical maps that correspond to a master equation in the Lindbald form. A theorem of Lindblad [39] and Gorini, Kossakowski and Sudarshan [40] proves a one-to-one correspondence between completely positive and trace preserving (CPTP) dynamical maps with the semi-group property and master equations in the Lindblad form. Consequently M. M. Wolf *et al.* have proposed using any deviation from the semi-group property as the principal characteristic of non-Markovian dynamical maps and constructed a quantitative measure of non-Markovianity as the minimal amount of isotropic noise that has to be added to the dynamics of an open quantum system to make it Markovian [44]. This definition is very severe and, in some cases, open to debate. There are dynamical processes that do not satisfy the semigroup property, but behave in a way that one would intuitively call Markovian.

To make this point more transparent, consider the microscopic derivation of the master equation *without* making the Markov approximation. The ensuing master equation has the same structure as the Lindblad master equation, but with time-dependent coefficients $\gamma_k = \gamma_k(t)$. As a result, the corresponding dynamical map is no longer time-homogenous and the semi-group property is violated. However, in the case when the decay rates are positive, $\gamma_k(t) \geq 0$ for each k and $t \geq t_0$, the dynamical map has the property of being *divisible*:

$$\Phi_{t_0,t} = \Phi_{t,s}\Phi_{s,t}, \text{ where } t \geq s \geq t_0. \tag{2.8}$$

The dynamical map can thus be concatenated into a collection of other dynamical maps and, analogously to the semi-group property, this concatenation has the intuitive interpretation of memoryless dynamics.

2.1.1 Non-Markovianity as indivisibility

If a Lindblad structured master equation with time-dependent rates has at least one decay rate that takes temporarily negative values, the divisibility of the corresponding dynamical map is broken. In this case the intermediate map $\Phi_{t,s}$ in the concatenation (2.8) is no longer completely positive. When a decay rate takes temporarily negative values the standard quantum jump picture breaks down due to the appearance of negative probabilities, and an extension thereof, the non-Markovian quantum jump method, becomes necessary [45]. According to this description, during a period of the decay rate being negative a previously occurred jump may be reversed. Reversed jumps recreate earlier states, advocating the idea of memory effects.

Constructing a measure of non-Markovianity based on indivisibility of the dynamical map is an idea put forward by several authors [16, 46–48]. The degree of non-Markovianity is quantified by the deviation of the intermediate map $\Phi_{t,s}$ from a completely positive map, which may be measured in several different ways. In this thesis I focus on the proposal of Rivas, Huelga and Plenio (RHP) [16], who exploit the Choi-Jamiolkowski isomorphism to construct a measure for non-Markovianity, based on indivisible dynamical maps. More specifically, the intermediate map $\Phi_{t,s}$ is CP if and only if the corresponding Choi matrix $(\Phi_{t,s} \otimes \mathbf{I}) |\Psi\rangle \langle\Psi|$ is positive ($|\Psi\rangle = \sum_{i=1}^{d} |i\rangle |i\rangle$ is a maximally entangled state), or, equivalently, if the trace norm of the Choi matrix is unity. Defining $t = s + \epsilon$ with ϵ infinitesimally small, the quantity

$$g(t) = \lim_{\epsilon \to 0^+} \frac{||(\Phi_{s+\epsilon,s} \otimes \mathbf{I}) |\Psi\rangle \langle\Psi| \,||_1 - 1}{\epsilon} \geq 0 \tag{2.9}$$

will vanish exactly when $\Phi_{s+\epsilon,s}$ is CP. Since formally $\Phi_{s+\epsilon,s} \to e^{\mathcal{L}_t \epsilon}$ as $\epsilon \to 0^+$, where $\mathcal{L}_t$ is the generator of the corresponding master equation, it is possible to make a second-order expansion in Eq. (2.9):

$$g(t) = \lim_{\epsilon \to 0^+} \frac{|| \left[\mathbf{I} + \epsilon(\mathcal{L}_t \otimes \mathcal{I})\right] |\Psi\rangle \langle\Psi| \,||_1 - 1}{\epsilon}, \tag{2.10}$$

and calculate the RHP measure directly from the master equation. This is a desirable property in cases when the exact solution, i.e., the dynamical map is not known. A time integral over $g(t)$ picks all the intervals when the dynamical map is indivisible and quantifies the degree of non-Markovianity in this sense. RHP further propose the normalized quantity

$$\mathcal{N}_{\text{RHP}} = \frac{\mathcal{I}_{\text{RHP}}}{\mathcal{I}_{\text{RHP}} + 1}, \quad \text{where} \quad \mathcal{I}_{\text{RHP}} = \int_{t_0}^{\infty} ds \; g(s), \tag{2.11}$$

as a measure of non-Markovianity, characterized by the property of indivisible dynamical map. For divisible maps $\mathcal{N}_{\text{RHP}} = 0$.

2.1.2 Non-Markovianity as information backflow

Divisible dynamical processes lead to monotonic decay of many important physical quantities [46]. The converse does not necessarily hold, but non-monotonic dynamics of these quantities can still be used to *witness* indivisibility. However, non-monotonic dynamics is often considered a signature of non-Markovian dynamics and, especially in the case when one may wish to harness the temporary revivals of these quantities in certain protocols, it is useful to *define* non-Markovian phenomena as deviations from such monotonic dynamics.

As an illustration of this approach, we consider here the seminal proposal of Breuer, Laine and Piilo (BLP) [17,18], where the quantity of interest is the distinguishability of two quantum states $\rho_{1,2}(t_0)$ evolving under the dynamical map $\Phi_{t_0,t}$. The distinguishability can be quantified using the trace norm as

$$D(t) = \frac{1}{2}||\rho_1(t) - \rho_2(t)||_1, \quad \rho_{1,2}(t) = \Phi_{t_0,t}\rho_{1,2}(t_0). \tag{2.12}$$

A divisible dynamical process decreases the distinguishability of the states monotonically, which can be interpreted as a continuous flow of information from the system to the environment. BLP define a dynamical process to be non-Markovian if it is possible to find a pair of initial states $\rho_{1,2}(t_0)$ such that the distinguishability increases for at least one interval of time $t_0 \leq a \leq t \leq b$, taking this to mean that information flows back to the system from the environment. Based on this idea, they define a measure for the degree of non-Markovianity in a dynamical process as

$$\mathcal{N}_{\text{BLP}} = \max_{\rho_{1,2}(t_0)} \int_{\sigma>0} ds\, \sigma(s), \quad \text{where} \quad \sigma(t) = \frac{dD(t)}{dt}, \tag{2.13}$$

and $\sigma(t)$ is called the information flow. Negative information flow signifies information loss from the system to the environment, while positive flux indicates a reversed flow of information. Thus the integration over all positive fluxes accumulates all the information that returns to the system for a given initial pair, and $\mathcal{N}_{\text{BLP}}$ captures the maximal amount of information that can return from the environment back to the system. The optimization over all pairs of initial states makes the measure complicated to compute,

although it has been shown that the two states maximizing the measure are on the boundary of the state space and orthogonal to each other [49]. Moreover, for some simple dynamical maps the maximizing pair has been found [50–52].

The BLP measure of non-Markovianity has been used extensively to study non-Markovian phenomena (see, e.g., [4, 5, 9, 25, 26, 53, 54]), but also other similar measures have been introduced. The measure has been generalized to continuous variable systems, where fidelity is used instead of the trace distance to describe distinguishability of two evolving states [55]. Lu, Wang and Sun measure information flux in terms of the Fisher information [56]. In this scenario one tries to estimate a given quantity, typically the phase of a state, after the state has been evolving under the action of a dynamical map. A lower bound on the variance of this estimate is given by the Fisher information, which decays monotonically when the dynamical map is divisible. Again, one may define non-Markovian processes as those that temporarily increase the Fisher information and integrate over all intervals of positive information flux to give a number quantifying the degree of non-Markovianity.

RHP propose studying the dynamics of a bipartite state comprising of the system evolving under the dynamical map of interest and coupled to a stationary ancilla state [16]. The bipartite system is initially in a maximally entangled state and when the dynamical map is divisible, entanglement decreases monotonically. Temporary increase of the entanglement can be interpreted as a non-Markovian effect. RHP propose using this scheme to witness entanglement, but one could envisage using an integration over all such time intervals as a measure of non-Markovianity. The system-ancilla correlations can also be measured by mutual information, like in Ref. [48]. Finally, in a similar spirit a very recent proposal studies the non-monotonic behavior of quantum and classical channel capacities, establishing a link between the non-Markovianity of a quantum channel and the maximal amount of quantum or classical information it can transmit [24].

2.2 Comparison of different approaches: Case study with damped driven qubit

Differences between the two distinctly different classes measures, one based on indivisibilty and the other on non-monotonic evolution of certain quantities, have been studied in Refs. [3, 57–60]. In Article III of this this thesis

we compare the BLP and the RHP measures of non-Markovianity for a simple but non-trivial physical process describing the evolution of a two-level atom (qubit) dissipating into a structured reservoir with a Lorenzian density function, while being simultaneously driven by a laser field. The microscopic derivation of the non-Markovian master equation, within the Born approximation, is presented in detail in Article I, and the dynamics of the qubit is studied in Article II. In this Section I review these articles with the main emphasis on Article III, and present some new results on the driven qubit model.

The dynamics of the damped driven qubit is characterized by three different time-scales [1, 2]. *Relaxation time-scale* τ_R is determined by the system-environment coupling. *Reservoir correlation time-scale* $\tau_C = \lambda^{-1}$ is the characteristic time-scale for non-Markovian phenomena and it is determined by the properties of the spectral density function, in this case the width of the Lorenzian λ. The narrower is the Lorenzian, the longer is the time-scale for non-Markovian effects. Finally, the *typical time-scale of the system* $\tau_S = (\Delta^2 + \Omega^2)^{-1/2}$ is given by $\Delta = \omega_0 - \omega_L$, the detuning between the two-level atom and the laser field and Ω, the Rabi frequency of the laser. In the weak coupling limit the relaxation time-scale is the longest time-scale for this model, much exceeding the reservoir correlation time $\tau_R \gg \tau_C$, while the typical time-scale interpolates between the two. In particular, τ_S can be either shorter or longer than the reservoir correlation time τ_C. We define parameter $p = \tau_C/\tau_S$ as the ratio between the last two time-scales and note that it can be modified by manipulating the laser parameters appropriately. This important parameter allows an interpolation between the *secular limit* $p \gg 1$, where we neglect a number of rapidly oscillating terms in the master equation, and the *nonsecular limit* $p \ll 1$ where these terms significantly affect the non-Markovian qubit dynamics. A second significant parameter $s = (\omega_0 - \omega_L)/\lambda$ describes the ratio between the atom-laser detuning and the width of the Lorenzian. Both play a crucial role in deciding the (non-)Markovianity of this model.

In the nonsecular limit the master equation has a Lindblad-like form (2.5) with a single time-dependent decay rate $\gamma(t)$. Quantity (2.10) is straightforward to calculate and gives $g(t) \propto P[\gamma(t)]$, where we define an auxiliary function $P(x) = 0,\ x \geq 0$ and $P(x) = -x,\ x < 0$. Divisibility is broken whenever $\gamma(t) < 0$. The complicated form of the corresponding jump operator A means that we are unable to find the solution of the master equation exactly, except when the atom and laser are on resonance $\Delta = 0$. This considerably complicates the calculation of the information flux of

(2.13). On resonance $\Delta = 0$ we find that $\sigma(t) \propto -\gamma(t)$ and therefore information flux is also reversed whenever $\gamma(t) < 0$. Numerical studies indicate that this result holds also for the off-resonant case and therefore we conclude that in the nonsecular limit $\mathcal{N}_{\mathrm{BLP}}$ and $\mathcal{N}_{\mathrm{RHP}}$ agree quantitatively. It is worth pointing out that this result is valid for *any* spectral density function. In the case of the Lorenzian spectrum $\gamma(t)$ takes temporarily negative values when $s \gtrsim 3.6$, and it is possible to cross from Markovian to non-Markovian dynamics by tuning the system parameters appropriately.

The differences between the the measures come to light in the secular regime. In this case the master equation has three Lindblad-like terms with time-dependent coefficients $\gamma_{0,\pm}(t)$, and unlike in the nonsecular case, the qubit dynamics is now analytically solvable. We find that

$$g(t) = \frac{1}{2}\left\{C_+^2 P[\gamma_+(t)] + C_-^2 P[\gamma_-(t)] + 4C_0^2 P[\gamma_0(t)]\right\}, \tag{2.14}$$

where $C_{0,\pm} = (s \pm p)/2p$ and $C_0 = \sqrt{p^2 + s^2}/2p$ are constant coefficients depending on parameters s and p. Now the divisibility property is broken whenever any of the three decay rates takes temporarily negative values. Information flux can also be calculated analytically:

$$\sigma(t) = -\frac{e^{-2\Lambda(t)}\Lambda'(t)(\delta x^2 + \delta y^2) + e^{-2\Gamma(t)}\Gamma'(t)\delta z^2}{2\sqrt{e^{-2\Lambda(t)}(\delta x^2 + \delta y^2) + e^{-2\Gamma(t)}\delta z^2}}, \tag{2.15}$$

where $\delta x = x_1(0) - x_2(0)$, $\delta y = y_1(0) - y_2(0)$, and $\delta z = z_1(0) - z_2(0)$ are the initial differences of the x-, y- and z- components of the Bloch vector representations of $\rho_1(0)$ and $\rho_2(0)$, respectively, at time $t_0 = 0$, and

$$\begin{aligned} \Gamma(t) &= \frac{1}{2}\int_0^t ds\left[C_+^2\gamma_+(s) + C_-^2\gamma_-(s) + 4C_0^2\gamma_0(s)\right], \\ \Lambda(t) &= \int_0^t ds\left[C_+^2\gamma_+(s) + C_-^2\gamma_-(s)\right]. \end{aligned} \tag{2.16}$$

Note again that these expressions hold for a generic spectral density function. The optimization needed to calculate $\mathcal{N}_{\mathrm{BLP}}$ is non-trivial, but owing to recent results of Ref. [49], it is now possible to refine equation (2.15) further. The condition that the maximizing states are on the boundary of the state space and orthogonal to each other, in the case of a qubit map, translates to the states being represented by Bloch vectors opposite to each other on the surface of the Bloch sphere. This simplifies the maximization

procedure considerably. Furthermore, the dynamics of the Bloch vector components, expressed explicitly as

$$\begin{aligned} x(t) &= e^{-\Gamma(t)}[x(0)\cos\omega t - y(0)\sin\omega t], \\ y(t) &= e^{-\Gamma(t)}[y(0)\cos\omega t + x(0)\sin\omega t)] \\ z(t) &= e^{-\Lambda(t)}\left\{z(0) + \int_0^t ds\, e^{\Lambda(s)}[C_-^2\gamma_-(s) - C_+^2\gamma_+(s)]\right\} \end{aligned} \tag{2.17}$$

shows circular symmetry in the xy-plane. Parametrizing initial states on the surface of the Bloch sphere in the usual way as $x_{1,2}(0) = \sin\theta_{1,2}\cos\phi_{1,2}$, $y_{1,2}(0) = \sin\theta_{1,2}\sin\phi_{1,2}$ and $z_{1,2}(0) = \cos\theta_{1,2}$, the circular symmetry of the dynamics means that we can fix a value for $\phi_{1,2}$. Choosing $\phi_{1,2} = 0$, and noting that the orthogonality of the pairs implies that $\theta_2 = \theta_1 + \pi$, information flux simplifies to

$$\tilde{\sigma}(t) = -\frac{e^{-2\Lambda(t)}\Lambda'(t)\sin^2\theta + e^{-2\Gamma(t)}\Gamma'(t)\cos^2\theta}{2\sqrt{e^{-2\Lambda(t)}\sin^2\theta + e^{-2\Gamma(t)}\cos^2\theta}}. \tag{2.18}$$

Maximization of the BLP measure of non-Markovianity then reduces to an optimization of $\int_{\tilde{\sigma}>0} ds\,\tilde{\sigma}(s)$ over $\theta \in [0, \pi/2]$. For this model the optimizing pair depends on the choice of the parameters s and p. As an example representing the deep secular regime we choose $p = 100$ and find the optimizing pair of states for a range of values of $s \in [0, 10]$. For small values of $s \leq 4.5$ the measure is optimized for antipodal states on the equator of the Bloch sphere ($\theta_1 = \pi/2$), whereas for $s > 4.5$ the optimal pair is the polar states ($\theta_1 = 0$). The optimal information flux is then

$$\sigma_{\rm opt}(t) = \begin{cases} -\Lambda'(t)e^{-\Lambda(t)}/2, & s \leq 4.5, \\ -\Gamma'(t)e^{-\Gamma(t)}/2, & s > 4.5. \end{cases} \tag{2.19}$$

The form of $\sigma_{\rm opt}(t)$ is distinctly different from $g(t)$ of Eq. (2.14). For some values of s the former depends only on $\gamma_\pm(t)$ while the latter is determined by all three decay rates. It is possible then, in principle, to have decay rates that lead to $g(t) > 0$ and $\sigma(t) < 0$, i.e., a scenario with an indivisible dynamical map but unidirectional information flow. This does not happen in the case of a Lorenzian spectrum, however, when we find that both measures are always strictly positive due to decay rates $\gamma_\pm(t)$ always having negative intervals. The two measures are shown explicitly in Fig. 2.1 as a function of parameter s. It is interesting to note that both measures have a jump for a certain values of s. For the RHP measure the jump at $s = 3.6$ coincides with decay rate $\gamma_0(t)$ starting to take negative values. In the case of the BLP measure the happens at $s = 4.5$ when the optimizing pair changes, and for $s \leq 4.5$ the BLP measure is insensitive to $\gamma_0(t)$.

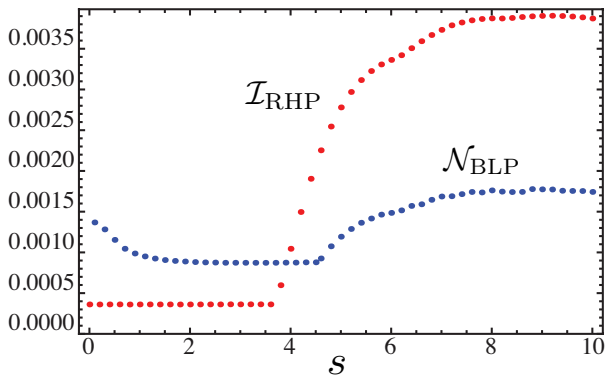

Figure 2.1: The non-Markovianity measures of RHP (Eq. (2.11), red dots) and BLP (Eq. (2.13), blue bots) for the driven qubit model in the secular regime, with $p = 100$, as a function of parameter s.

Chapter 3

Purely dephasing non-Markovian dynamics

Using the toolbox of non-Markovian open quantum systems introduced in the previous Chapter it is possible to evaluate non-Markovian phenomena systematically and assess their impact in applications. In this Chapter I introduce a physical model of a qubit dephasing in a bosonic reservoir and show how it can be used to study some fundamentally interesting open questions on non-Markovian dynamics. More specifically, I will study the origin of memory effects for the pure dephasing model and demonstrate how they can be exploited to prolong the transition from classical to quantum decoherence indefinitely.

3.1 Microscopic origin of non-Markovianity

Non-Markovianity is often associated to structured reservoirs, i.e., models where the spectral density function $J(\omega)$ characterizing the system-environment coupling varies appreciably with frequency. For the driven qubit of the previous Chapter, for example, non-Markovian effects take place only when the width of the Lorenzian is narrow enough in the nonsecular regime. In the secular regime the dynamics is always non-Markovian, and decreasing the width leads to a higher degree of non-Markovianity. A similar result has been reported for the Jaynes-Cummings model: the more structure the reservoir has, the more pronounced are the memory effects [52]. In Article VI we show, however, that the connection between spectral densities and non-Markovianity is more subtle in the case of purely dissipative dynamics.

The connection between non-Markovianity and structured spectra can be established using a very general dephasing model [61–63]. The Hamiltonian for this model describing the interaction between a qubit and a bosonic reservoir is

$$H = \omega_0 \sigma_z + \sum_k \omega_k a_k^\dagger a_k + \sum_k \sigma_z (g_k a_k + g_k^* a_k^\dagger), \tag{3.1}$$

where ω_0 is the qubit frequency, ω_k the frequencies of the k-th reservoir modes, a_k ($a_k^\dagger$) are the annihilation (creation) operators and g_k describes the coupling constant between the k-th reservoir mode and the qubit. In the limit of a continuum of modes the coupling constants are replaced by the reservoir spectral density function

$$J(\omega) = \sum_k |g_k|^2 \delta(\omega_k - \omega). \tag{3.2}$$

This model admits an exact solution (see Refs. [61–63]) with constant diagonal elements of the qubit and off-diagonal elements decaying as $\rho_{ij}(t) = e^{-\Gamma(t)} \rho_{ij}(0)$, $i \neq j$. The dephasing factor describing this decay for an environment in thermal equilibrium at temperature T is

$$\Gamma(t) \;=\; 2 \int_0^\infty d\omega \, J(\omega) \coth\left(\frac{\hbar\omega}{2k_B T}\right) \frac{1 - \cos(\omega t)}{\omega^2}, \tag{3.3}$$

corresponding to a master equation of the form

$$\frac{d\rho(t)}{dt} = \frac{\gamma(t)}{2} \left[\sigma_z \rho(t) \sigma_z - \frac{1}{2} \left\{ \sigma_z \sigma_z, \rho(t) \right\} \right]. \tag{3.4}$$

Here the time-dependent dephasing rate is

$$\gamma(t) = \frac{d\Gamma(t)}{dt}. \tag{3.5}$$

It has been shown that for this dynamical process the pair of initial states optimizing the measure of Eq. (2.13) is any pair of antipodal states on the equator of the Bloch sphere [50, 51]. Without a loss of generality we may choose the initial pair to be $\rho_1(0) = |+\rangle\langle+|$ and $\rho_2(0) = |-\rangle\langle-|$, where $|\pm\rangle = (|1\rangle \pm |0\rangle)/\sqrt{2}$. For this optimal choice the distinguishability (which for qubit states is half the Euclidian distance of the corresponding Bloch vectors) is

$$D_{\text{opt}}(t) = e^{-\Gamma(t)}, \tag{3.6}$$

leading to optimised information flux

$$\sigma_{\rm opt}(t) \;\; = \;\; \frac{dD_{\rm opt}(t)}{dt} = -\gamma(t)e^{-\Gamma(t)}. \tag{3.7}$$

The qubit dynamics is non-Markovian ($\sigma_{\rm opt}(t) > 0$ for some interval of time) if and only if the dephasing rate takes temporarily negative values, $\gamma(t) < 0$. During these intervals the divisibility property is violated and information flows from the environment back to the system as manifested in temporary increase in the distinguishability of the initial states.

With the exact solution in terms of the spectrum at hand we can formulate a condition for the spectral density to induce non-Markovian dynamics of the qubit. A strictly positive dephasing rate corresponds to monotonic dynamics of the dephasing factor $\Gamma(t)$. Since the cosine transform of a convex function increases monotonically, we can deduce that a sufficient condition for Markovianity for this dephasing model is that the quantity

$$\xi(\omega, T) \equiv J(\omega) \coth\left[\hbar\omega/2k_BT\right]/\omega^2 \tag{3.8}$$

is a convex function of ω. Furthermore, this condition turns out to be also necessary if we specify the study to the family of Ohmic spectra

$$J(\omega) = \frac{\omega^s}{\omega_c^{s-1}} e^{-\omega/\omega_c}, \tag{3.9}$$

where ω_c is the reservoir cutoff frequency and s is the so-called *Ohmicity parameter*. The Ohmicity parameter determines if the spectrum is sub-Ohmic ($0 < s < 1$), Ohmic ($s = 1$) or super-Ohmic ($s > 1$). For the Ohmic class of spectra the dephasing rate can be calculated analytically in the zero-T and high-T limits:

$$\gamma(t) = \begin{cases} \omega_c[1+(\omega_c t)^2]^{-s/2}\Xi[s]\sin\left[s\arctan(\omega_c t)\right], & T = 0 \\ 2k_BT[1+(\omega_c t)^2]^{-(s-1)/2}\Xi[s-1]\sin\left[(s-1)\arctan(\omega_c t)\right], & \text{high-T}, \end{cases} \tag{3.10}$$

where $\Xi[x]$ is the Euler gamma function. It is easy to check that $\gamma(t)$ takes temporarily negative values in the zero-T case when $s > 2$ and in the high-T case when $s > 3$, and to confirm that the quantity $\xi(\omega, T)$ is non-convex exactly for the same values. The intermediate-T case cannot be studied analytically, but numerical studies suggest that transition of the dynamics from Markovian to non-Markovian coincides exactly with the $\xi(\omega, T)$-function turning from convex to non-convex. Therefore we conclude that the convexity of $\xi(\omega, T)$ is a necessary and sufficient condition for the Ohmic class of spectral density functions.

Physically the dephasing process can be understood as follows. The action of the qubit on the environment is a state-dependent displacement operation on each mode of the environment. The two states of the qubit excite each mode with opposite phases and this leads to an overlap between the states of the mode in each case. Destructive interference between excitations of a mode at different times leads to recoherences at the frequency of that mode. The balance between these two effects determines whether the dynamics is Markovian or not. In the case of the Ohmic class of spectra, convexity of $\xi(\omega, T)$ not only guarantees that decoherence outweighs recoherence, but it is required. This highlights the key role of the low frequency part of the spectrum in the occurrence of information backflow. The full scope of this statement becomes evident in Ch. 4, where I discuss a physical implementation of the dephasing model in a set-up with a more complex spectral density function than the one of Eq. (3.9). I will show how dramatically the low-frequency part of the spectrum controls the crossover from Markovian to non-Markovian dynamics and give an example of a system where a highly structured spectrum fails to induce non-Markovian dynamics.

3.2 Harnessing non-Markovianity: Time-invariant discord

In this Section I discuss an interesting consequence of non-Markovian dephasing dynamics. It is known that for some systems that non-Markovian effects can prolong the existence of quantum properties. Generally noise from the environment tends to destroy quantum properties of a system and a drastic example of this is a phenomenon known as entanglement sudden death, i.e., a total loss of entanglement of a bipartite system in a finite time [64]. The scenario is more optimistic when the dynamics of the bipartite system is characterized by memory effects and entanglement can be temporarily revived even after it has been lost [65]. In the remaining part of this Chapter I show how non-Markovianity can combat and even prevent the detrimental effect of the environment on a more general type of quantum correlation known as *quantum discord* [32].

Entanglement captures only a part of the quantum correlations shared by a bipartite system. The total amount of quantum correlations is given by quantum discord, originally introduced by Ollivier and Zurek [30], and independently by Henderson and Vedral [31]. Quantum discord is defined

as the difference between two expressions of mutual information that agree in the classical domain but deviate for quantum states. It can be non-zero even for separable states, therefore describing quantum correlations exceeding entanglement. The topology of the set of zero-discord states is markedly different from the set of separable states. The former has measure zero and is nowhere dense [66], while the latter has a finite volume. Consequently quantum discord can vanish only asymptotically, i.e., without a sudden death [67, 68]. Furthermore, discord is more resilient against environmental noise than entanglement, as demonstrated by Mazzola *et al.* in Ref. [69]. The authors studied a two-qubit system under the influence of local Markovian dephasing channels and unveiled a class of initial states for which quantum discord is *unaffected* by decoherence for a finite time $\bar{t}$.

Remarkably, using a non-Markovian model we show in Article VI that the time $\bar{t}$ can be extended to infinity; *discord is time-invariant*. In other words, the dynamics of the two-qubit system for the total evolution time is characterized by a decay of classical correlations, while quantum correlations are permanently frozen to their initial value. The lack of a transition from classical decoherence (decay of classical correlations) to quantum decoherence (decay of quantum correlation) can be traced back to the failure of the Markov approximation.

We consider a system of two qubits A and B dephasing in their own local reservoirs. The noise on each qubit is described by the master equation of Eq. (3.4) and we assume the Ohmic class of spectra, leading to decay rates of Eq. (3.10). The qubits are prepared in an initial state of the form

$$\rho_{AB} = \frac{(1+c)}{2} \left|\Psi^{\pm}\right\rangle \left\langle\Psi^{\pm}\right| + \frac{(1-c)}{2} \left|\Phi^{\pm}\right\rangle \left\langle\Phi^{\pm}\right|, \tag{3.11}$$

where $|\Psi^{\pm}\rangle = (|00\rangle \pm |11\rangle)/\sqrt{2}$ and $|\Phi^{\pm}\rangle = (|01\rangle \pm |10\rangle)/\sqrt{2}$ are the four Bell states and $|c| < 1$. Quantum discord $\mathcal{Q}(\rho_{AB})$ of a bipartite state ρ_{AB} can be formulated as the difference between the mutual information $\mathcal{I}(\rho_{AB})$ and the classical correlations $\mathcal{C}(\rho_{AB})$ which, for the initial class of states of Eq. (3.11), dephasing in the Ohmic reservoir, take the form

$$\begin{aligned} \mathcal{I}[\rho_{AB}(t)] &= \sum_{j=1}^{2} \frac{1+(-1)^j c}{2} \log_2[1+(-1)^j c] \\ &+ \sum_{j=1}^{2} \frac{1+(-1)^j e^{-\Gamma(t)}}{2} \log_2[1+(-1)^j e^{-\Gamma(t)}] \end{aligned} \tag{3.12}$$

and

$$\mathcal{C}[\rho_{AB}(t)] = \sum_{j=1}^{2} \frac{1+(-1)^j\chi(t)}{2} \log_2[1+(-1)^j\chi(t)], \tag{3.13}$$

where $\chi(t) = \max\{e^{-\Gamma(t)}, c\}$, and we have taken $c > 0$ for simplicity. Quantity $\chi(t)$ now dictates whether the dynamics is characterized by quantum or classical decoherence and this, in turn, is determined by the values of the Ohmicity parameter s and the initial value parameter c. If a time $\bar{t}$ exists such that equation

$$e^{-\Gamma(\bar{t})} = c \tag{3.14}$$

has a solution, then for $t < \bar{t}$ the discord is constant while classical correlations decay, and after $t = \bar{t}$ discord starts to decay. This is the scenario studied in Ref. [69].

For the family of Ohmic spectra, however, we discover a range of values of s for which Eq. (3.14) has no solution and the transition time $\bar{t}$ does not exist. It is for this range of values of s that only classical correlations are affected by noise, leading to classical decoherence, while discord remains frozen forever. The landscape of the values of s and c leading to the phenomenon of time-invariant discord for zero-T reservoirs is shown in Fig. 3.1. We also show the dynamics of quantum and classical correlations for two exemplary parameter choices. For the first pair $c = 0.1,\ s = 1$ the transition time exists, while for the second pair $c = 0.1,\ s = 2.5$ we observe the phenomenon of time-invariant discord. Note that the value of the frozen discord, $\mathcal{Q} = (1+c)\log_2(1+c)/2 + (1-c)\log_2(1-c)/2$, increases with the value of c. Hence time-invariant discord is most pronounced for large values of c, corresponding to $2 \lesssim s \lesssim 3$ and coinciding with the dynamics of the individual qubits being non-Markovian.

Let us now discuss the connection between time-invariant discord and non-Markovianity in more detail. The existence of this phenomenon can be traced back to the failure of the Markov approximation. First note that, strictly speaking, it is not even possible to make the Markov approximation for the model in question. Imposing the limit $t \to \infty$ on the decay rate (3.10) gives $\gamma(t) \to 0$, i.e., the decay rate has no Markovian counterpart. However, for some values of s the qubit dynamics is well approximated by a master equation of the form of (3.4), where the decay rate is a positive constant $\gamma(t) \simeq \gamma_{\text{eff}} \geq 0$, which we may interpret as an effective Markovian decay rate. The decoherence factor is then $\Gamma_{\text{eff}}(t) = \exp[-\gamma_{\text{eff}}t]$, and Eq. (3.14) has always a solution $\bar{t} = -\ln(|c|)/(2\gamma_{\text{eff}})$; there is a transition from

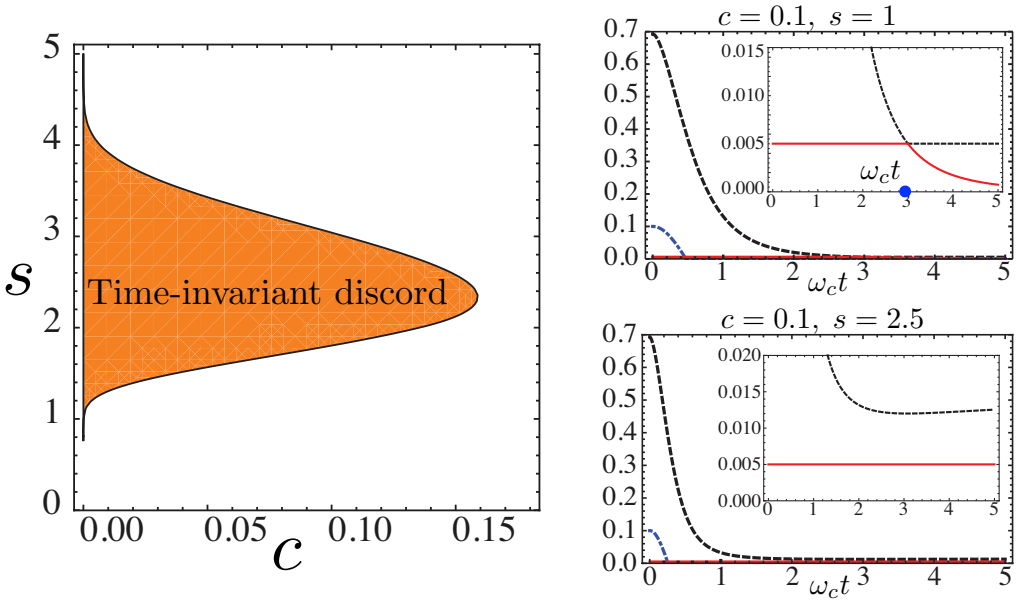

Figure 3.1: On the left hand side figure the shaded region marks range of parameters s and c for which the discord is frozen forever for $T = 0$. Outside this region one will always observe a transition from classical to quantum decoherence. The right hand side figures show an example of each with quantum discord (solid red line), classical correlations (dashed black line) and entanglement measured by concurrence [70] (dot-dashed blue line). For $c = 0.1,\ s = 1$ the system has a sudden transition from quantum to classical decoherence: the blue dot points the transition time $\bar{t}$. For $c = 0.1,\ s = 2.5$, instead, discord is frozen forever.

classical to quantum decoherence. For a range of parameters $1 \lesssim s \lesssim 4$ this effective Markovian description fails, since $\Gamma(t)$ tends to a finite value in the limit $t \to \infty$. It is exactly the existence of this finite value that leads to Eq. (3.14) having no solution, and consequently to discord being frozen forever.

Chapter 4

Physically realizable model of a controllable non-Markovian process

The previous Chapter discussed the origin of non-Markovian dynamics for a general dephasing qubit model and presented an interesting consequence of non-Markovianity on the evolution of quantum and classical correlations. For the family of Ohmic spectra the emergence of non-Markovian effects and the subsequent phenomenon of time-invariant discord relied on the ability to control the Ohmicity parameter s: below a temperature-dependent critical value of s the dynamics was shown to be Markovian and only increasing its value introduced memory effects in the qubit evolution. Moreover, a significant amount of time-invariant discord was discovered only for a limited range of parameter s. This raises the natural question whether such a controllable dephasing model could be found in Nature, or if the prediction of Ch. 3 are merely a theoretical curiosity.

In this Chapter I introduce a physical model which simulates the dephasing model introduced in the previous Chapter using a set-up of ultracold quantum gases. Building on the original proposal of Ref. [71], we have shown in Article IV that the effective Ohmicity parameter in this model can be controlled to a very high degree in an experimentally feasible way. In Articles V and VII we further demonstrate that the ultracold realization of the dephasing model is robust against thermal noise and that this is a feature specific to the particular qubit architecture we consider. This experimentally realistic, precisely controllable and remarkably robust model makes an ideal testbed for the observation of fundamental phenomena such

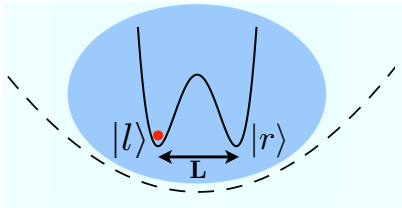

Figure 4.1: Impurity atom (red dot) trapped in a double well potential (solid line), surrounded by a Bose-Einstein condensed ultracold gas of a different species (blue area) trapped in a shallow potential (dashed line).

as the crossover from Markovian to non-Markovian dephasing in the case of a single qubit, and time invariant discord for two qubits.

4.1 The model

Consider two ultracold gases of different species A and B trapped in optical potentials $V_A(\mathbf{x})$ and $V_B(\mathbf{x})$, respectively. Potential $V_A(\mathbf{x})$ has a very specific form: it consists of a row of deep double well potentials and the ultracold gas of species A is assumed to be so scarce that only a single atom occupies each double well. A single atom in the double well forms a qubit system with the two qubit states represented by the occupation of the atom in the left or the right well. Potential $V_B(\mathbf{x})$, instead, forms a shallow trap for species B, which is then cooled to a Bose-Einstein condensed (BEC) state. The BEC acts as an environment for the double well qubit, or conversely, the atoms trapped in the double well are impurities in the BEC, as shown in Fig. 4.1. The two different species have a density-density interaction and the Hamiltonian for this system is a sum of the Hamiltonians describing the impurity atoms, the background gas and their interaction,

$$\begin{aligned} H_A &= \int d\mathbf{x}\, \Psi^\dagger(\mathbf{x}) \left[\frac{\mathbf{p}_A^2}{2m_A} + V_A(\mathbf{x}) \right] \Psi(\mathbf{x}), \\ H_B &= \int d\mathbf{x}\, \Phi^\dagger(\mathbf{x}) \left[\frac{\mathbf{p}_B^2}{2m_B} + V_B(\mathbf{x}) + \frac{g_B}{2} \Phi^\dagger(\mathbf{x})\Phi(\mathbf{x}) \right] \Phi(\mathbf{x}), \\ H_{AB} &= \frac{g_{AB}}{2} \int d\mathbf{x}\, \Phi^\dagger(\mathbf{x})\Psi^\dagger(\mathbf{x})\Psi(\mathbf{x})\Phi(\mathbf{x}), \end{aligned} \tag{4.1}$$

respectively. Here m_A, $\Psi(\mathbf{x})$ and $V_A(\mathbf{x})$ are the mass, field operator and the trapping potential of the impurity atom, m_B, $\Phi(\mathbf{x})$, $g_B = 4\pi\hbar^2 a_B/m_B$

and $V_B(\mathbf{x})$ are the mass, field operator, coupling constant and the trapping potential of a background gas atom and a_B is the scattering length of the boson-boson collisions. Finally, $g_{AB} = 4\pi\hbar^2 a_{AB}/m_{AB}$ is the coupling constant of the impurity-boson interaction where $m_{AB} = m_A m_B/(m_A + m_B)$ is the effective mass.

After a series of approximations the total Hamiltonian takes a form resembling that of Eq. (3.1). More specifically, we expand the impurity field operator in terms of Wannier functions $\{\phi_{\mathbf{k}}\}$ localised in the two wells of the double well potential. Assuming sufficiently deep wells both hopping and tunnelling are suppressed, and the Wannier functions take a Gaussian form. We assume that the background gas is weakly interacting and can be treated in the usual Bogoliubov approximation, neglect all terms that are quadratic in the creation and annihilation operators of the Bogoliubov modes and assume that the background gas is homogenous. The interaction Hamiltonian determining the qubit dynamics, up to a possible phase, is then

$$H_{AB} = \frac{g_{AB}\sqrt{n_0}}{\Omega} \sum_{\mathbf{k},\, p=L,R} \hat{n}_p\, \hat{c}_k \sqrt{\frac{\epsilon_{\mathbf{k}}}{E_{\mathbf{k}}}} \int d\mathbf{x}\, |\phi(\mathbf{x}_p)|^2 e^{i\mathbf{k}\cdot\mathbf{x}} + H.c. \quad (4.2)$$

where n_0 is the condensate density, Ω is the quantisation volume, $E_{\mathbf{k}} = \sqrt{\epsilon_{\mathbf{k}}(\epsilon_{\mathbf{k}} + 2n_0 g_B)}$ is the Bogoliubov dispersion relation, $\epsilon_{\mathbf{k}} = \hbar^2 k^2/(2m_B)$ is the dispersion relation of a non-interacting gas with $k = |\mathbf{k}|$, and $\hat{c}_k$ is the Bogoliubov excitation operator. Operator $\hat{n}$ is the number operator of the impurities. When there is exactly one impurity atom in the double well system $\hat{n}_R = \frac{1}{2}(1 + \sigma_z)$ and $\hat{n}_L = \frac{1}{2}(1 - \sigma_z)$, where $\sigma_z = |l\rangle\langle l| - |r\rangle\langle r|$. The two wells are spatially separated by distance $\mathbf{L}$ so that $\mathbf{x}_R = \mathbf{x}_L - \mathbf{L}$.

The dynamics of a single qubit can be solved analytically [71]. Exactly as in the decoherence model of Chapter 3, the qubit dephases with $\rho_{ij}(t) = e^{-\Gamma(t)}\rho_{ij}(0)$, $i \neq j$. The decoherence factor specific to this set-up is

$$\Gamma(t) = 8 g_{AB}^2 n_0 \sum_{\mathbf{k}} (|u_k| - |v_k|)^2 e^{-k^2\sigma^2/2} \frac{\sin^2(E_k t/2\hbar)}{E_k^2} \coth\left(\frac{\beta E_k}{2}\right) \sin^2(\mathbf{k}\cdot\mathbf{L}), \quad (4.3)$$

where σ is the ground state parameter of the double well, $|u_k|$ and $|v_k|$ are the k-th Bogoliubov modes and $\beta = 1/k_B T$. Note that the decoherence factor is dependent on the dimension of the BEC. This can be altered experimentally by changing the relative strengths of the optical potential $V_B(\mathbf{x})$ in the three axial directions. Stronger confinement in one axial direction creates a flat pancake BEC with effective dimension two. Similarly strong

confinement in two axial directions creates an effectively 1-dimensional, cigar shaped BEC. Another experimentally feasible way of regulating the qubit dynamics by changing the properties of the environment is provided by Feshbach resonances. This technique can be used to control the scattering length a_B of the background gas particles very precisely and enables an extrapolation from a free background gas to an interacting background gas. The latter regime is especially attractive from a fundamental perspective. Most studies on open quantum systems focus on non-interacting environments and it is interesting to see the effect of an interacting environment on the emergence of non-Markovianity in the qubit dynamics.

We consider a ^{87}Rb-condensate of density $n_3 = n_0 = 10^{20}\mathrm{m}^{-3}$ and ^{23}Na impurity atoms trapped in an optical lattice with lattice wavelength $\lambda =$ 600nm and trap parameter $\sigma = 45$nm. The well separation is $L = \lambda/8$. The impurity-boson coupling is fixed by setting the corresponding scattering length to $a_{AB} = 55\,a_0$, where a_0 is the Bohr radius. In the case of a 3D environment the boson-boson coupling frequency is $g_B^{3D} = 4\pi\hbar^2 a_B/m_B$ but now we assume that the s-wave scattering length of the background gas can be tuned from its natural value $a_B = a_{Rb} = 99\,a_0$ via Feshbach resonances. We explore a range of values of a_B consistent with the assumption of dilute gas and with the regime of weakly interacting gases. The latter is a stronger condition, requiring $\sqrt{a_B^3 n_0} \ll 1$. As a consequence, we can tune the scattering length up to a maximum value given by $a_B \approx 3\,a_{Rb}$. The boson-boson coupling frequency is slightly modified for lower dimensions. In the quasi-2D case the scattering length is still much smaller than the axial length of the condensate, $a_B \ll a_z$, and the coupling term is modified to $g_B^{2D} = \sqrt{8\pi}\hbar^2 a_B/(m_B a_z)$ with 2D condensate density $n_2 = \sqrt{\pi} n_0 a_z$ [72]. Within the limits of a dilute gas we can increase the scattering length up to $a_B \approx 2\,a_{Rb}$. The potential $V_B(\mathbf{x})$ can be also modified to create a cigar-shaped quasi-1D background gas with transversal width $a_\perp$. The consequent coupling is $g_B^{1D} = 2\hbar^2 a_B/(m_B a_\perp^2)$ and the 1D density is $n_1 = n_0 \pi a_\perp^2$, again provided that gas is weakly enough confined, $a_B \ll a_\perp$ [73]. In the quasi-1D regime diluteness of the gas allows at most $a_B \lesssim a_{Rb}$.

4.1.1 Crossover from Markovian to non-Markovian

Recall that for purely dephasing qubit evolution is in the class of processes for which the pair maximizing the BLP measure is known [50,51]: it is a pair of antipodal states on the equator of the Bloch sphere. This means that the BLP measure can be studied analytically. For a realistic set of parameters

describing the ultracold gases there is at most only a single period when the decay rate $\gamma(t) = \Gamma'(t)$ is negative, signifying non-Markovianity in the sense of both indivisibility and information backflow. This enables the use of a modified non-Markovianity measure

$$\mathcal{N} = \frac{e^{-\Gamma(b)} - e^{-\Gamma(a)}}{e^{-\Gamma(0)} - e^{-\Gamma(a)}}, \quad a \leq t \leq b \Leftrightarrow \Gamma'(t) > 0, \tag{4.4}$$

which captures the ratio of information returning to the system during interval $a \leq t \leq b$ to the information lost from the system to the environment in the previous interval $0 \leq t \leq a$. Unlike the original BLP measure, the modified quantifier (4.4) is bounded between zero (system only leaks information) and one (system regains all previously lost information) and is therefore more meaningful as a number.

The non-Markovianity measure (4.4) for the parameter values elaborated above is shown in Fig. 4.2 in the case of a zero-T reservoir. In all three dimensions the dynamics of the impurity qubit is Markovian for a free or a very weakly interacting background gas, and non-Markovian for a sufficiently large boson-boson interaction of the background gas. The specific critical value of the boson-boson scattering length signifying the crossover from Markovian ($\mathcal{N} = 0$, $a_B \leq a_B^{\text{crit}}$) to non-Markovian ($\mathcal{N} > 0$, $a_B \geq a_B^{\text{crit}}$) dynamics depends only on the dimensionality of the BEC: $a_B^{\text{crit, 3D}} \approx 0.034\, a_{Rb} < a_B^{\text{crit, 2D}} \approx 0.122 a_{Rb} < a_B^{\text{crit, 1D}} \approx 0.183 a_{Rb}$.

The ultracold realization of the dephasing model shows a crossover from Markovian to non-Markovian dynamics with a suitable manipulation of experimentally feasible parameters. The demonstration of this crossover was initially shown in Article IV of this Thesis for a zero-T reservoir and in Article VI we extended this analysis to a finite-T reservoirs to show that the qubit model we consider is robust enough against thermal fluctuations to retain the crossover for experimentally realistic temperatures. The measure, as a function of the background scattering length, is shown for two finite temperatures in Fig. 4.2. Only at higher temperatures of about $T = 100$ nK the thermal fluctuations start washing out non-Markovian effects, turning the qubit dynamics Markovian. Resilience against thermal fluctuations and the ability to create non-Markovian dynamics with a suitable dimension of the BEC combined with a strong enough boson-boson interaction is a feature characteristic to the double well qubit architecture, as will be demonstrated in the next Section by comparing this model to an atomic quantum dot model.

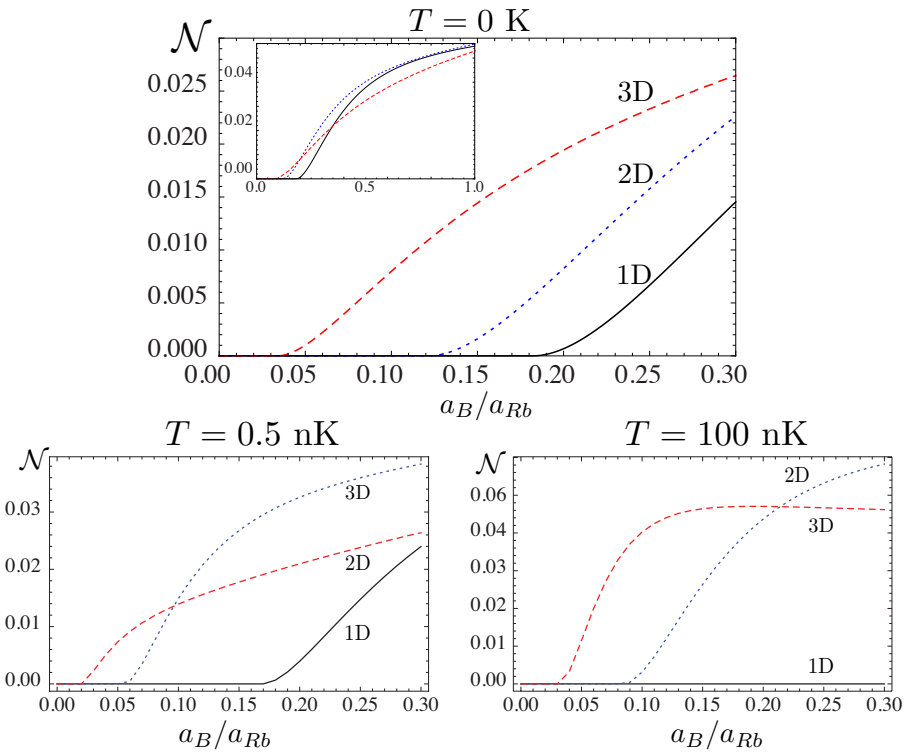

Figure 4.2: Top figure: Non-Markovianity measure $\mathcal{N}$ as a function of the scattering length of the background gas a_B when the background gas is three dimensional (red dashed line), quasi-two dimensional (blue dotted line) and quasi-one dimensional (black solid line) and $T = 0$K. The inset shows a longer range of the scattering length a_B/R_{Rb}. Bottom figures: The same for $T = 0.5$nK and $T = 100$nK.

4.1.2 Comparison to AQD

The double well architecture is only one way to realize the pure dephasing model using ultracold gases. A model proposed is Refs. [74,75] replaces the double well qubit with a single impurity atom trapped in a deep harmonic potential and takes two internal states of the atom as the qubit states (See Fig. 4.3). Otherwise the set-up is identical to the model already presented. This model is referred to as the atomic quantum dot and its total Hamiltonian is also given by Eq. (4.1). With the same assumptions and approximations as before the impurity-environment interaction Hamiltonian and the corresponding decoherence factor for the atomic quantum dot

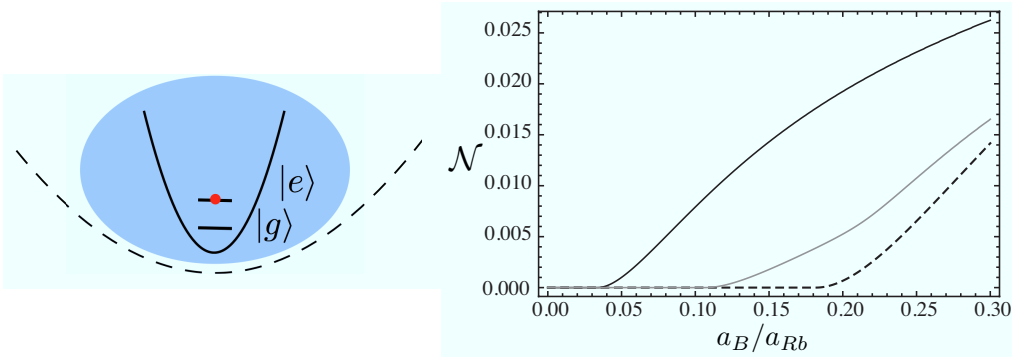

Figure 4.3: Model of an atomic quantum dot and its non-Markovianity measure as a function of the the background scattering length $a_B/a_{\rm Rb}$ for a zero-T reservoir (solid black line) and a $T = 10$nK reservoir (solid gray line). Dashed black line shows for comparison the non-Markovianity of the double well qubit in a zero-T reservoir.

model are

$$\begin{aligned} H_{AB} &= \frac{g_{AB}\sqrt{n_0}}{\Omega}\sum_{\mathbf{k}} \hat{n}\,\hat{c}_k\sqrt{\frac{\epsilon_{\mathbf{k}}}{E_{\mathbf{k}}}}\int d\mathbf{x}|\phi(\mathbf{x})|^2 e^{i\mathbf{k}\cdot\mathbf{x}} + H.c., \\ \Gamma(t) &= \frac{g_{AB}^2 n_0}{\Omega}\sum_{\mathbf{k}} e^{-k^2\sigma^2/2}\frac{\epsilon_{\mathbf{k}}}{E_{\mathbf{k}}}\frac{\sin^2(\frac{E_{\mathbf{k}}t}{2\hbar})}{E_{\mathbf{k}}^2}. \end{aligned} \tag{4.5}$$

The similarity between these expressions and those of the double well qubit model is significant. The latter depends on the spatial separation between the two wells of the double well, and it turns out that this spatial separation has a crucial impact on the non-Markovian dynamics of the dephasing model.

Figure 4.4 shows the dynamics of the decoherence factor for the two different qubit models. In the cases of two and three dimensional environments the decoherence factors evolve in a similar way, but for the quasi-1D BEC there is a striking dissimilarity in the dephasing process; the double well qubit is almost unaffected by environmental noise (decoherence factors converges quickly to a very small value), while the atomic quantum dot dephases completely (decoherence factor grows without bound), tending to a maximally mixed state. Moreover, the non-Markovian properties of the two models, manifested as non-monotonic dynamics of the decoherence factor, are very different. Dynamics of the atomic quantum dot is Markovian in

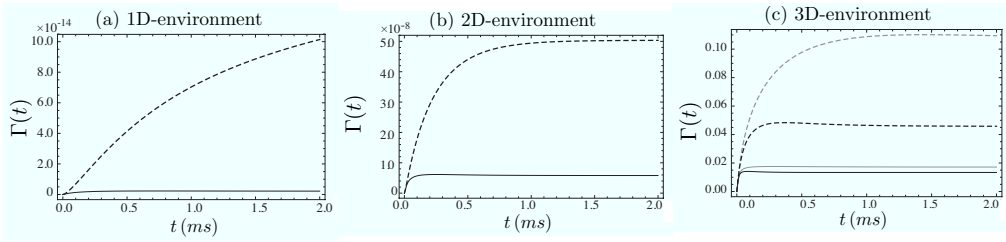

Figure 4.4: The decoherence function $\Gamma(t)$ for the double well qubit (solid lines) and the atomic quantum dot model (dashed lines) for (a) one-dimensional, (b) two-dimensional and (c) three-dimensional BEC environments and for background scattering length values $a_B = 0.25a_{\mathrm{Rb}}$ (black lines) and $a_B = a_{\mathrm{Rb}}$ (gray lines).

the quasi-1D and quasi-2D cases and only when the environment is a three dimensional BEC we are able to find a critical value of the scattering length such that there is a crossover from Markovian to non-Markovian dynamics. This is in stark contrast with the double well model which has the crossover in all three dimensions. Moreover, non-Markovian effects in the dynamics of the atomic quantum dot model are not robust against thermal noise. As shown in Fig. 4.3, a temperature which slightly reduces the amount of non-Markovianity in the dynamics of the double well model washes out all memory effects for the atomic quantum dot.

4.1.3 Spectral density function

As shown in Chapter 3, the crossover from Markovian to non-Markovian dynamics for pure dephasing dynamics can be traced back to the behaviour the spectral density function. Indeed, the differences between the two different physical models of qubit dephasing presented here become transparent when analyzing their spectra. Moreover, a comparison of the two spectra underlines the immense importance of the low-frequency part of the spectral density function.

For these physical models the form of the spectral density functions is more complicated than the phenomenological spectrum (3.9) of the general dephasing model. The low frequency part of each spectra, however, is well approximated by an Ohmic type dependence on the frequency, $J(\omega) \propto \omega^{s_{\mathrm{eff}}}$. The effective Ohmicity parameter s_{eff} depends on the model parameters and turns out to be especially sensitive to the dimensionality of the BEC

environment and the boson-boson scattering length a_B; increasing either of these experimentally controllable parameters increases the value of s_{eff} (See Fig. 4.5). Crucially, with suitable choice of parameters the value of s_{eff} is sufficiently large to induce non-Markovian effects, exactly as in the general dephasing model. For both qubit models in a zero-T environment the parameters leading to $s_{\text{eff}} \gtrsim 2$ correspond to the qubit dephasing in a non-Markovian way. When thermal effects are taken into account, a larger threshold value has to be reached. For a given set of parameters the value of s_{eff} for the double well qubit is always larger than for the atomic quantum model, explaining why the former model is more non-Markovian than the latter.

As conjectured before, it is the low frequency part of the spectral density function that dictates whether the dynamics of the system is Markovian or not. The extent of this statement becomes evident when we look at the whole spectrum in Fig. 4.5. The spectral density function of the double well qubit model has a very rich structure over the whole range of relevant frequencies, especially in the case of a 1D environment. Contrary to the typical idea that structured spectra are associated to non-Markovian effects, for dephasing dynamics this structure has no effect on the non-Markovianity. If $s_{\text{eff}} \lesssim 2$, as determined by a small enough scattering length a_B, the qubit dynamics is still Markovian despite the rich structure over the whole range of relevant frequencies. This result highlights the importance of the low frequency part of the spectrum in the emergence of non-Markovian dynamics and emphasizes the difference between pure dephasing dynamics and models such as the driven qubit or the Jaynes-Cummings model, where structured spectra can be associated to memory effects.

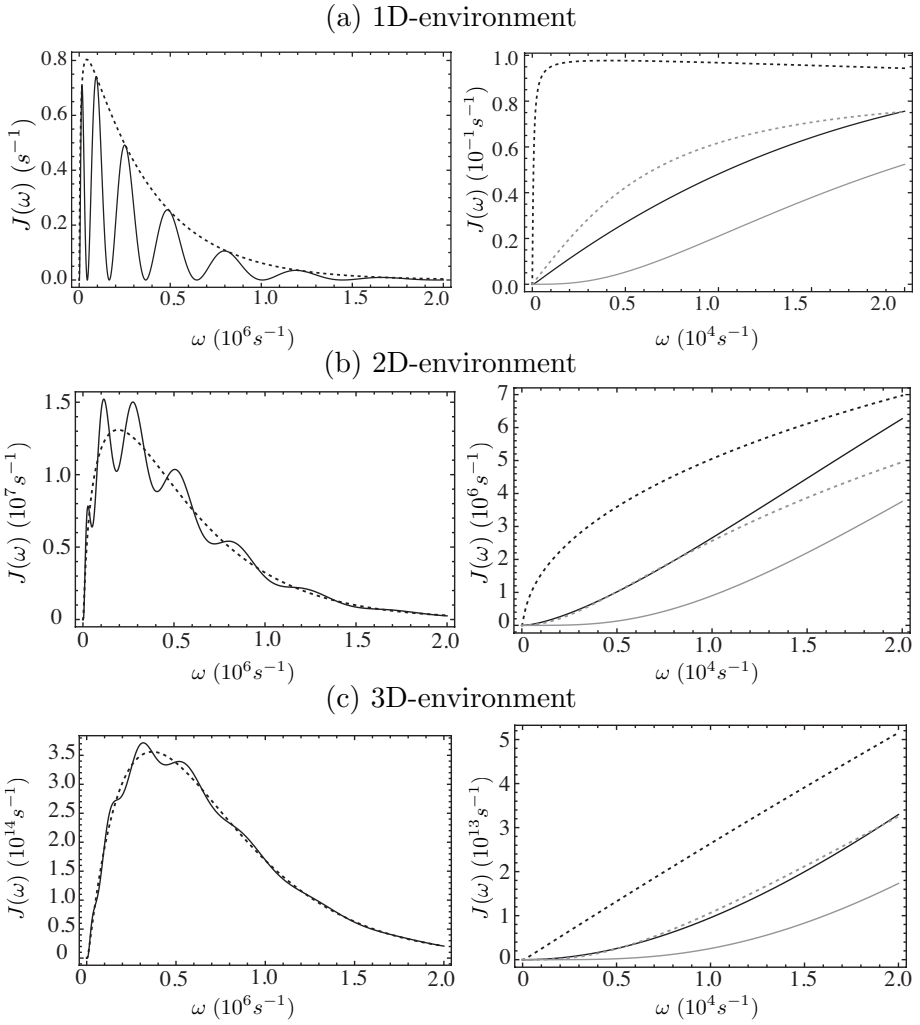

Figure 4.5: Spectral density functions $J(\omega)$ for the double well model (solid lines in all figures) and the atomic quantum dot model (dashed lines in all figures) in a (a) one-dimensional, (b) two-dimensional and (c) three-dimensional environment. Left hand side figures show the full spectrum, and the figures on the right show the low-frequency contribution. In the latter we show the spectrum for a weakly interacting background gas with $a_B = 10^{-3} a_{Rb}$ (black lines) and for a BEC with $a_B = a_{Rb}$ (gray lines).

Chapter 5

Probe qubits

The archetype of open quantum systems, i.e., a small system of interest interacting with a larger environment, lends itself to an alternative viewpoint. If we are interested, instead, in the larger system, can we infer some of its properties by studying the smaller system? In this picture the smaller system acts as a *probe* of the larger system. Evolution of the probe system is dictated by the properties of the environment and the way the two are coupled, and with a suitable set-up a given property of the environment can be exposed by some feature in the evolution of the probe. In a best-case-scenario this property can be studied without significantly affecting the larger system in the spirit of making a non-destructive measurement of the environment. In this Chapter I present some results addressing this idea, based on Articles V and IX of this Thesis.

5.1 Probing the Loschmidt echo

Consider once again a purely dephasing open system model, where a qubit is coupled to a complex many-body environment via an interaction term H_I [5]. Assume an initially factorized composite state

$$\rho_{SE}(0) = |\phi_S\rangle\langle\phi_S| \otimes \rho_E(0) \tag{5.1}$$

with a pure initial system $|\phi_S\rangle = c_g|g\rangle + c_e|e\rangle$, $|c_g|^2 + |c_e|^2 = 1$. The evolution of the environment is consequently split into two branches with weights given by the qubit coefficients c_α, $\alpha = g, e$, so that in each branch the environment Hamiltonian H_E is replaced by an effective Hamiltonian

$$H_\alpha = H_E + \langle\alpha| H_I |\alpha\rangle . \tag{5.2}$$

Here the latter term represents the action of the qubit on the environment described by the interaction Hamiltonian. Tracing over the environmental degrees of freedom we find that the qubit evolves as

$$\rho_S(t) = |c_g|^2|g\rangle\langle g| + |c_e|^2|e\rangle\langle e| + c_g^* c_e\, \nu(t)|e\rangle\langle g| + \text{H.c.}, \tag{5.3}$$

where $\nu(t)$ is the decoherence factor. When also the initial environmental state is pure, $\rho^E(0) = |\Phi\rangle\langle\Phi|$, the decoherence factor is simply the overlap between perturbed environmental states of the two branches

$$\nu(t) = \langle\Phi|e^{iH_g t}e^{-iH_e t}|\Phi\rangle. \tag{5.4}$$

The square modulus of the decoherence factor

$$|\nu(t)|^2 = L(t) \tag{5.5}$$

is a quantity known as the Loschmidt echo. Loschmidt echo describes the stiffness of a many-body system to external perturbations and it emerges in many interesting fields of study [35]. In the context of chaotic systems, for example, the Loschmidt echo is used to study the sensitivity of dynamics on the initial state. It also characterizes the ability of a system to return to its initial state after imperfect backwards evolution, thus having consequences on the study of time reversal. Indeed, the concept of Loschmidt echo was originally coined after extensive discussions between Loschmidt and Boltzmann on the origin of macroscopic irreversibility.

In this case we obtain the Loschmidt echo of the many-body environment directly from the qubit evolution. Further, information flow between the system and the environment is determined by the Loschmidt echo. More explicitly, the distinguishability of a pair of antipodal states on the equator of the Bloch sphere, i.e. the pair maximizing the BLP measure of non-Markovianity for dephasing noise, is $D[\rho_s^1(t), \rho_s^2(t)] = \sqrt{L(t)}$. Hence any non-monotonic behavior of the Loschmidt echo immediately indicates a reversed information flux. This gives a neat expression for the measure of non-Markovianity in terms of the Loschmidt echo:

$$\mathcal{N} = \sum_n \sqrt{L(b_n)} - \sqrt{L(a_n)}, \tag{5.6}$$

where $[a_n, b_n]$ are the time intervals over which $dL(t)/dt > 0$ and $L(a_n)$ and $L(b_n)$ are the local minimum and maximum, respectively, of the Loschmidt echo. Note that for this model many other characterizations on non-Markovianity mutually agree and information flowback appears hand in

hand with revered Fisher information flux, revivals of entanglement with an ancilla and indivisibility of the dynamical map. The utility of this simple connection between the non-Markovianity measure and the Loschmidt echo becomes transparent when the environment is a critical system.

5.2 Ising model in a transverse field

Ising model in a transverse field is a prototype of a quantum critical system. This simple and intuitive model comprises of a 1D chain of spins with nearest neighbor interactions, characterized by parameter J, and under the influence of a transverse magnetic field with interaction strength λ. The Hamiltonian for this system is

$$H_{\text{Ising}} = -J \sum_j \sigma_j^z \sigma_{j+1}^z + \lambda \sigma_j^x. \tag{5.7}$$

In the limit of $\lambda \ll J$ the system has a doubly degenerate ferromagnetic ground state, where all the spins point in a single direction, either up or down. In the opposite limit $\lambda \gg J$ the magnetic field dominates the spin-spin interactions and the system has a paramagnetic ground state with all the spins polarized in the direction of the magnetic field. When the two competing effects balance, $\lambda = J$, the transverse Ising model undergoes a second order quantum phase transition.

We propose to probe the phase transition of the transverse Ising model with a central spin, which couples to all the spins in the Ising chain with equal strength δ. The interaction Hamiltonian is

$$H_I = \delta |e\rangle\langle e| \sum_j \sigma_j^x. \tag{5.8}$$

The central qubit splits the evolution of the transverse Ising model into two branches. In the branch corresponding to the qubit in the ground state the Ising chain evolves according to Hamiltonian (5.7), while in the other branch the strength of the magnetic field is replaced by an effective value $\lambda^* = \lambda + \delta$; the presence of the qubit effectively increases the impact of the transverse field.

It has been shown previously that the decay of the Loschmidt echo is strongly enhanced around the critical point [76]. The hyper-sensitivity of the Loschmidt echo to the critical point translates in a striking way to the non-Markovianity measure, which is shown in Fig. 5.1. When the

magnetic field is tuned in such a way that the Ising model is not at the critical point, the dynamics of the central qubit is always non-Markovian and at least a small amount of information returns temporarily from the system to the environment. The closer the Ising model is to the critical point, the less information is returned to the system. However, it is *only at the critical point* when the information flow is unidirectional. An especially interesting feature is the independence of the result $\mathcal{N} = 0$ on the size of the environment. This implies that the rapid, monotonic decay of the Loschmidt echo at the critical point, leading to a Markovian qubit dynamics could be a universal feature of this model. This currently open question would be interesting to study in the future.

Let us note that since the Loschmidt echo of the transverse Ising model does not have an analytical expression in the thermodynamic limit, we can only study the non-Markovianity measure for a finite number of environment spins. Consequently the echo will always have revivals arising from finite-size effects and the qubit dynamics is trivially non-Markovian. Fortunately in many cases it is possible to distinguish different physical phenomena happening on different time-scales, e.g., in this case the revivals due to finite-size effects and the revivals due to the structure of the environment. In Fig. 5.1 the time-integration of the non-Markovianity measure has been truncated to a time smaller than the expected reoccurrence time and hence the measure captures revivals due to information flowback.

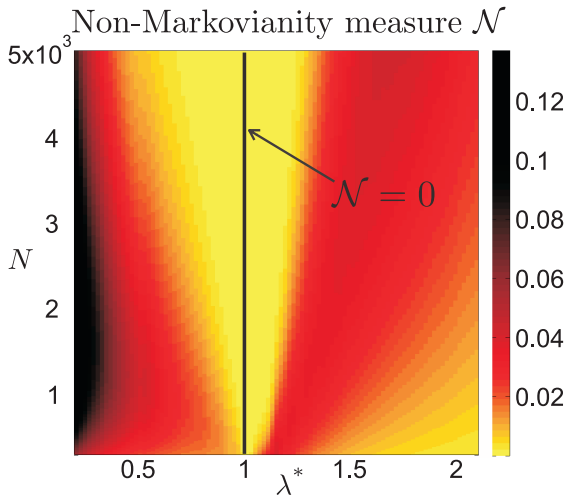

Figure 5.1: Non-Markovianity measure $\mathcal{N}$ as a function of the particle number N and the renormalized field λ^* for $J = 1$.

5.3 Coulomb chain

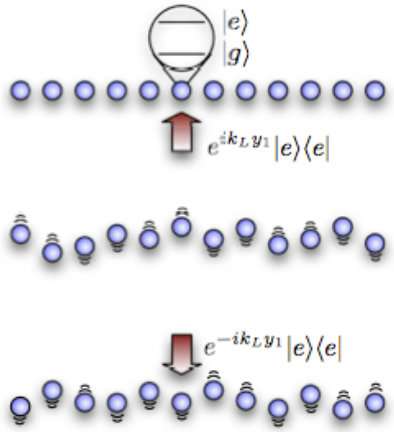

Figure 5.2: Ramsey interferometry on a Coulomb chain. Reprinted from Ref. [79] with the kind permission of Gabriele De Chiara.

The ability of a probe qubit to pinpoint the quantum phase transition of its environment is not unique to the model introduced above. In Article IX we study a set-up where the non-Markovianity measure characterizing the dynamics of a probe qubit clearly indicates the phase transition of a many-body system.

The system in question is a Coulomb chain of repulsively interacting ions in an anisotropic trap with a large transverse confinement, cooled to very cold temperatures where quantum fluctuations dominate the system properties. With sufficiently strong confinement in the transverse direction the ions form a linear array. If the transverse confinement is reduced or the density of the ions in the chain is increased, the chain undergoes a structural phase transition to a zigzag structure. The precise nature of the structural linear-zigzag phase transition is still unresolved, but there is increasing evidence that it is a quantum phase transition [77], and of the same universality class as the transverse Ising model [78].

It has been proposed that this structural phase transition can be observed using Ramsey interferometry on one of the ions in the Coulomb chain [79]. In this scheme, shown in Fig. 5.2, a transverse laser pulse excites the modes of the Coulomb chain, and the ion is left to evolve freely with the rest of the chain. After a time t a second laser pulse of the oppo-

site direction is imposed on the probe ion, and the ground state probability $P_g(t)$ is then measured. The ground state probability now depends on the properties of the external degrees of freedom, namely the state of the Coulomb chain, and its evolution is distinctly different for a chain in the linear configuration and for a chain in the zigzag configuration.

The Ramsey interferometry scenario readily admits an open system picture where the two internal degrees of freedom of the ion excited in the Ramsey sequence play the role of a qubit and the excitation modes of the kicked Coulomb chain are the environmental degrees of freedom. The dynamical map describing the dynamics of the qubit system is very complex, including the effect of the two laser pulses of the Ramsey interferometry and the intermediate unitary evolution of the Coulomb chain. In Article IX we showed that the qubit dissipates and dephases under the effect of this dynamical map and characterized the degree of non-Markovianity of the map as a function of a tunable parameter describing how far the Coulomb chain is from the critical point of the structural phase transition.

For this dynamical map we resorted to a numerical evaluation of the pair of states maximizing the BLP measure of non-Markovianity since an analytical result for complicated dissipative dynamics is not known. Compelling numerical evidence indicates that the maximizing pair is the same as for the dephasing model, namely $|+\rangle$ and $|-\rangle$. Interestingly, this pair of states is not affected by dissipative dynamics and undergoes pure dephasing dynamics only, making the situation intriguingly similar to the transverse Ising model probed by a centrally coupled qubit. The distinguishability of the optimal pair of states and the consequent non-Markovianity measure depend explicitly on the visibility of the Ramsey interferometry signal, a quantity reminiscent of the Loschmidt echo describing the evolution of the overlap of two environment states.

The sensitivity of the environment to perturbations close to the critical point, now measured by the visibility, is again manifested beautifully in the non-Markovian character of the probe qubit. However, the relationship between the criticality of the Coulomb chain and the non-Markovianity measure is more complex than in the case of the transverse Ising model. In particular, there is now a greater sensitivity to the time truncation in the integration of the BLP measure, as shown in Fig. 5.3. For short evolution times the non-Markovianity measure has a distinct minimum at the critical point. Unlike in the case of the transverse Ising model the measure does not go to zero at the critical point indicating a total inhibition of information backflow, but nonetheless the reversed flow of information

is clearly suppressed.

If the truncation is made after a longer period of time, the dependence of the non-Markovianity measure on the deviation from criticality is rather different: now the measure has a *maximum* at the critical point (See Fig. 5.3). This is explained by a specific feature of the long-time dynamics, namely the system coupling dominantly to only a single "soft" mode of the environment. Coupling to only a single environment mode creates a strong interaction between the mode and the probe qubit leading to considerable bidirectional information exchange and a high value of the non-Markovianity measure. This effect is enhanced the closer the system is to the critical point, explaining why the measure has a maximum at the critical point. Despite having a more complicated dependence on the time truncation than the probe for the transverse Ising model, the probe we use to detect the structural phase transition of the Coulomb chain is remarkably sensitive to the critical point of the ion chain.

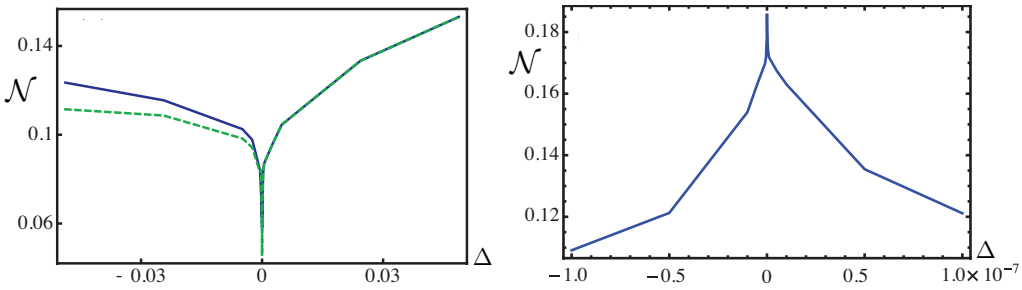

Figure 5.3: Left: Non-Markovianity measure $\mathcal{N}$ of the Coulomb chain for short time-scale truncation as a function of Δ for $N = 100$ (blue solid line) and $N = 1000$ (green dashed line). $\Delta = \nu_t/\nu_c - 1$ is a parameter characterizing how much the transverse trap frequency ν_t deviates from the critical value ν_c. When $\Delta < 0$ the chain has the linear structure and when $\Delta > 0$ it is found in the zig-zag structure. Right: Non-Markovianity measure $\mathcal{N}$ of the Coulomb chain for long time-scale truncation as a function of Δ for $N = 300$.

Chapter 6

Concluding remarks

This Thesis has discussed three aspects of the theory on non-Markovian open quantum systems, namely what non-Markovianity is, when and why does it emerge and what are the consequences of non-Markovian memory effects. Addressing the first question is pivotal when considering the latter two, although the main emphasis of this Thesis has been the causes and consequences of non-Markovian phenomena.

In the first part of the Thesis I introduced some prevailing definitions on non-Markovianity and compared them in a qubit model where the qubit is simultaneously driven by a laser field and damped by a non-trivially structured reservoir. This study sheds light on the subtly different ways of defining memory effects as well as on the microscopic processes that induce non-Markovian dynamics for this specific model.

An important model in this Thesis has been the purely dephasing qubit model. I have discussed it in a very general setting to prove a simple condition for a reservoir spectrum to induce non-Markovian qubit dynamics and to introduce the phenomenon of time-invariant discord. I have also demonstrated that a set-up of ultracold quantum gases realizes the dephasing model with an Ohmic type spectral density function in an experimentally realistic, robust and highly controllable way.

In the last part of the Thesis I have proposed a protocol to probe some properties of a complex many-body environment using a non-Markovian probe qubit. This scheme was shown to be very efficient in detecting a phase transition in two different physical models, an Ising model in a transverse field, the prototype of a second order quantum phase transition, and a 1D Coulomb chain undergoing a structural phase transition from a linear to a zig-zag structure.

Bibliography

[1] P. Haikka, Phys. Scr. T **140**, 014047 (2009).

[2] P. Haikka and S. Maniscalco, Phys. Rev. A **81,** 052103 (2010).

[3] P. Haikka, J. D. Cresser and S. Maniscalco, Phys. Rev. A **83**, 012112 (2011).

[4] P. Haikka, S. McEndoo, G. De Chiara, M. Palma and S. Maniscalco, Phys. Rev. A **84**, 031602(R) (2011).

[5] P. Haikka, J. Goold, S. McEndoo, F. Plastina and S. Maniscalco, Phys. Rev. A **85**, 060101(R) (2012).

[6] P. Haikka, S. McEndoo, G. De Chiara, M. Palma and S. Maniscalco, Phys. Scr. T **151**, 014060 (2012).

[7] P. Haikka, T. H. Johnson and S. Maniscalco, Phys. Rev. A **87**, 010103(R) (2013).

[8] P. Haikka, S. McEndoo and S. Maniscalco, Phys. Rev. A **87**, 012127 (2013).

[9] M. Borrelli, P. Haikka, G. De Chiara and S. Maniscalco, Submitted for publication, arXiv:1302.4260.

[10] S. McEndoo, P. Haikka, C. De Chiara, G. M. Palma and S. Maniscalco, Europhys. Lett. **101**, 60005 (2013).

[11] C. Addis, P. Haikka, S. McEndoo, C. Macchiavello and S. Maniscalco, Phys. Rev. A **87**, 052109 (2013).

[12] H. P. Breuer and F. Petruccione, The *Theory of Open Quantum Systems*, (Oxford Univ. Press, 2007).

[13] U. Weiss, *Quantum Dissipative Systems*, 3rd ed. (World Scientific, Singapore, 2008).

[14] C.W. Gardiner and P. Zoller,*Quantum Noise* (Springer- Verlag, Berlin, 2010).

[15] M. A. Schlosshauer, *Decoherence and the Quantum-To-Classical Transition* (Springer-Verlag, Berlin, 2007).

[16] A. Rivas, S. F. Huelga and M. B. Plenio, Phys. Rev. Lett. **105**, 050403 (2010).

[17] H.-P. Breuer, E.-M. Laine and J. Piilo, Phys. Rev. Lett. **103**, 210401 (2009).

[18] E.-M. Laine, J. Piilo and H-P. Breuer, Phys. Rev. A **81**, 062115 (2010).

[19] L. Mazzola, E.-M. Laine, H.-P. Breuer, S. Maniscalco, and J. Piilo, Phys. Rev. A **81**, 062120 (2010); E.-M. Laine, K. Luoma, and J. Piilo, Jour. Phys B **45**, 154004 (2012).

[20] S. F. Huelga, A. Rivas, M. B. Plenio, Phys. Rev. Lett. **108**, 160402 (2012).

[21] A. W. Chin, S. F. Huelga and M. B. Plenio, Phys. Rev. Lett. **109**, 233601(2013).

[22] R. Vasile, S. Olivares, M. G. A. Paris, and S. Maniscalco, Phys. Rev. A **83**, 042321 (2011).

[23] E.-M. Laine, H.-P. Breuer and J. Piilo, arXiv:1210.8266

[24] B. Bylicka, D. Chruscinshi and S. Maniscalco, arXiv:1302.2585v1

[25] García-Mata, C. Pineda, and D. Wisniacki, Phys. Rev. A **86**, 022114 (2012).

[26] M. Žnidarič, C. Pineda, and I. García-Mata, Phys. Rev. Lett. **107**, 080404 (2011).

[27] M. Thorwart, J. Eckel, J. H. Reina, P. Nalbach, S. Weiss, Chem. Phys. Lett. **478**, 234 (2009).

[28] G. R. Fleming, S. F. Huelga, and M. B. Plenio, New J. Phys. **13**, 115002 (2011).

[29] B.-H. Liu *et al.* arXiv:1208.1358; J.-S. Tang *et al.* Europhys. Lett. **97**, 10002 (2012) ; B.-H. Liu *et al.*, Nature Physics **7**, 931 (2011).

[30] H. Ollivier and W. H. Zurek, Phys. Rev. Lett. **88**, 017901 (2001).

[31] L. Henderson and V. Vedral, J. Phys. A **34**, 6899 (2001).

[32] K. Modi, A. Brodutch, H. Cable, T. Paterek, and V. Vedral, Rev. Mod. Phys. **84**, 1655 (2012).

[33] M. F. Cornelio *et al.*, Phys. Rev. Lett. **109**, 190402 (2012)

[34] W. H. Zurek, Phys. Rev. D **24**, 1516 (1981). W. H. Zurek, *ibid* **26**, 1862 (1982). W. H. Zurek, Rev. Mod. Phys. **75**, 715 (2003).

[35] A. Goussev *et al.*, Scholarpedia, 7(8) 11687 (2012), arXiv:1206.6348.

[36] W. F. Stinespring. Proc. Amer. Math. Soc. **6** 211 (1955).

[37] S. Nakajima, Prog. Theor. Phys. **20**, 948 (1958); R. Zwanzig, J. Chem. Phys. **33**, 1338 (1960).

[38] F. Shibata, Y. Takahashi and N. Hashitsume, J. Stat. Phys. **17**, 171 (1977).

[39] G. Lindblad, Comm. Math. Phys. 48, **119** (1976)

[40] V. Gorini, A. Kossakowski, E.C.G. Sudarshan, J. Math. Phys. **17**, 821 (1976).

[41] J. Dalibard, Y. Castin and K. Mølmer, Phys. Rev. Lett. **68**, 580 (1992).

[42] M. B. Plenio and P. L. Knight, Rev. Mod. Phys. **70**, 101 (1998).

[43] M. M. Wolf and J. I. Cirac, Commun. Math. Phys. **279**, 147 (2008).

[44] M. M. Wolf, J. Eisert, T. S. Cubitt, and J. I. Cirac, Phys. Rev. Lett. **101**, 150402 (2008).

[45] J. Piilo, S. Maniscalco, K. Härkönen, and K.-A. Suominen, Phys. Rev. Lett. **100**, 180402 (2008); J. Piilo, K. Härkönen, S. Maniscalco, and K.-A. Suominen, Phys. Rev. A **79**, 062112 (2009).

[46] D. Chruscinshi and A. Kossakowski, J. Phys. B: At. Mol. Opt. Phys. **45**, 154002 (2012).

[47] S. C. Hou, X. X. Yi, S. X. Yu and C. H. Oh, Phys. Rev. A **83**, 062115 (2011).

[48] S. Luo, S. Fu and H. Song, Phys. Rev. A **86**, 044101 (2012).

[49] S. Wissmann, A. Karlsson, E.-M. Laine, J. Piilo, and H.-P. Breuer, Phys. Rev. A **86**, 062108 (2012).

[50] Z. Y. Xu, W. L. Yang and M. Feng, Phys. Rev. A **81**, 044105 (2010).

[51] Z. He, J. Zou, L. Li, and B. Shao, Phys. Rev. A **83**, 012108 (2011).

[52] J.-G. Li, J. Zou and B. Shao, Phys. Rev. A **81**, 062124 (2010). Phys. Rev. A **83**, 012108 (2011).

[53] T. J. G. Apollaro, C. Di Franco, F. Plastina, and M. Paternostro Phys. Rev. A **83**, 032103 (2011).

[54] G. Clos and H.-P. Breuer, Phys. Rev. A **86**, 012115 (2012).

[55] R. Vasile, S. Maniscalco, M. G. A. Paris, H.-P. Breuer, and J. Piilo, Phys. Rev. A **84**, 052118 (2011).

[56] X. M. Lu, X. Wang and C. P. Sun, Phys. Rev. A. **82**, 042103 (2010).

[57] D. Chruscinshi, A. Kossakowski and A. Rivas, Phys. Rev. A **83**, 052128 (2011).

[58] H.-S. Zeng, N. Tang, Y.-P. Zheng, and G.-Y. Wang, Phys. Rev. A **84**, 032118 (2011).

[59] F. Benatti, R. Floreanini and S. Olivares, Phys. Lett. A **45** 2951 (2012).

[60] H.S. Zeng, N. Tang, Y.P. Zheng and T.T. Xu, Eur. Phys. Jour. D **66**, 255 (2012).

[61] J. Luczka, Physica A **167**, 919 (1990).

[62] G. M. Palma, K.-A. Suominen, and A. K. Ekert, Proc. R. Soc. London, Ser. A **452**, 567 (1996).

[63] J. H. Reina, L. Quiroga and N. F. Johnson, Phys. Rev. A **65**, 032326 (2002).

[64] T. Yu and J. H. Eberly, Phys. Rev. Lett. **93**, 140404 (2004); **97**, 140403 (2006).

[65] L. Mazzola, S. Maniscalco, J. Piilo, K.-A. Suominen, and B. M. Garraway, Phys. Rev. A **79**, 042302 (2009).

[66] A. Ferraro, L. Aolita, D. Cavalcanti, F. M. Cucchietti, and A. Acín, Phys. Rev. A **81**, 052318 (2010).

[67] T. Werlang, S. Souza, F. F. Fanchini, and C. J. Villas Boas, Phys. Rev. A **80**, 024103 (2009).

[68] F. F. Fanchini, T. Werlang, C. A. Brasil, L. G. E. Arruda, and A. O. Caldeira, Phys. Rev. A **81**, 052107 (2010).

[69] L. Mazzola, J. Piilo and S. Maniscalco, Phys. Rev. Lett. **104**, 200401 (2010).

[70] W. K. Wootters, Phys. Rev. Lett. **80**, 2245 (1998).

[71] M. A. Cirone, G. De Chiara, G. M. Palma and A. Recati, New Jour. Phys. **11** 103055 (2009).

[72] L. Pitaevskii and S. Stringari, *Bose-Einstein Condensation* (Oxford University Press, Oxford, 2003).

[73] I. Bloch, J. Dalibard, and W. Zwerger, Rev. Mod. Phys. **80**, 885 (2008).

[74] A. Klein, M. Bruderer, S. Clark and D. Jaksch, New J. Phys. **9**, 411(2007).

[75] M. Bruderer, A. Klein, S. Clark and D. Jaksch, Phys. Rev. A **76** 011605(R) (2007).

[76] H. T. Quan *et al.*, Phys. Rev. Lett. **96**, 140604 (2006).

[77] E. Shimshoni, G. Morigi, and S. Fishman, Phys. Rev. Lett. **106**, 010401 (2011).

[78] P. Silvi, G. De Chiara, T. Calarco, G. Morigi, and S. Montangero, arXiv:1301.3386v1.

[79] G. De Chiara, T. Calarco S. Fishman and G. Morigi, Phys. Rev. A **78**, 043414 (2008)